Semester Project

Development of a Signal Processing Board for N-Pulse's EMG Bracelet Project

Lausanne, June 2025

Student : Julien Thévenoz (326772)

Supervisor : Prof. Alexandre Schmid

Ecole Polytechnique Fédérale de Lausanne

Contents

Introduction

N-Pulse is a new student association dedicated to biomedical technology whose main project this year is the development of an open-source bionic prosthetic hand for people who have lost their lower forearm [1]. The prosthesis should be controlled in a way which is as intuitive and natural for the user as possible.
As such different paths are being investigated : EMG, brain-computer interfaces and computer vision, with the most focus on detection of EMG signals in the upper forearm to estimate the desired hand position.

Myoelectric signals are the small voltage changes produced in muscle fibers during contraction of the skeletal muscles. These signals can be captured by sensors placed either inside the muscle tissue (intramuscular electrodes) or on the surface of the skin (surface electrodes). The recording and interpretation of the myoelectric signals is called electromyography (EMG) and is a well-established technique in medical practice commonly used to help with neuromuscular disorder diagnosis [2].

Since most muscles moving the hand are located in the forearm, surface-electrode electromyography (sEMG) can also be applied to the forearm and combined with machine learning techniques to estimate hand gestures [3] and even finger-specific movements [4]. This application of EMG technology is a growing field in biomedical research [5] due to its potential for medical research and prostheses development, but also in the tech and gaming industry where it is examined as an alternative to traditional keyboard and controllers (Meta has recently unveiled their EMG wristband prototype for augmented reality [6]).

In the autumn semester 2024, a semester project aiming to develop the first version of a surface EMG bracelet for N-Pulse was carried out by the two founders of the association[7]. Based on a design by researchers of the Politecnico di Torino university [7][8], they created custom signal acquisition modules and the mechanical design for the bracelet, and did preliminary research towards developing custom processing hardware but due to time constraints they selected the commercial Rasperry Pi Zero 2W board to process the signals and run the classification algorithm using three electrode channels.

The present semester project was proposed by N-Pulse in the 2025 spring semester as a follow-up on their progress, continuing work on the EMG Bracelet by developing a custom printed circuit board (PCB) to replace the Raspberry Pi board.
It is supervised by Professor Alexandre Schmid, head of the Biomedical and Neuromorphic Microelectronic Systems research group (BNMS).

Goals

The aim of this semester project is to develop a PCB able to decode the signals provided by the EMG signal acquisition modules to run an on-board machine learning algorithm for hand gesture detection (which is developed by the association's software team). This board (named the Signal Processing board) is a part of N-Pulse's EMG Bracelet project, which aims to develop a standalone, wearable, lightweight and open-source bracelet for hand gesture estimation.
Although it is mainly conceived to be inside of the bracelet, it may eventually be directly integrated in N-Pulse's robotic hand prosthesis further down the line.
According to the desired specifications of the EMG Bracelet, the Signal Processing Board should be able to receive 16 EMG signals simultaneously, power the signal acquisition modules which provide them, run the ML algorithm and transmit the results over wireless or wired communication.
The design process and resulting PCB should be well documented and open source, such as to allow other members of N-Pulse or anyone interested in similar projects to easily replicate and improve the product.

State of the Art

Different wireless electromyography armbands aimed towards hand gesture recognition have been developed for research purposes and as commercial products, but not many of them have enough available information to quantify their performance.

In 2022, Mongardi et al [9] integrate and extend their previous sEMG sensor [8] in a complete EMG bracelet capable of very low-power live analysis and wireless transmission of the hand-gesture prediction and the data used for the prediction simultaneously. Their system can classify 9 hand positions with a latency of less than 132 ms (130ms acquisition time, 1.34ms inference time) and an accuracy of almost 92% using an on-board Artifical Neural Network classifier. The bracelet itself has seven EMG channels, Bluetooth Low-Energy communications and current absorption of only 2.92mA, giving it an estimated operating time of 60 hours. Their microcontroller unit has 1MB of Flash memory, 384 kB of RAM and 48 MHz clock speed.

To reduce computation and thus energy consumption, they use an event-driven feature extraction technique called Average Threshold Crossing (ATC), which consists of counting the mean amount of times an EMG signal surpasses a given threshold in a determined time window. Even though it is a significantly less complex signal than the complete EMG signal, this ATC parameter is a strong indicator of muscle activity and allows Mongardi et al to predict hand-gestures with a high accuracy (≈92%). The strong advantage is that the ATC techniques requires to store and manipulate significantly less data, requiring only a single number for each time window instead of the whole discretized EMG signal.

The most widespread EMG product is the MYO Armband produced by Thalmic Labs from 2014 to 2019 [10], [11], [12]. It contains 8 EMG sensors and a 9-axis inertial measurement unit (IMU), has Bluetooth Low-Energy 4.0 capability and an integrated battery rechargeable through a micro-USB port. Through a combination of EMG and orientation/acceleration analysis, the software developed by Thalmic Labs allows the detection of five hand gestures: fist, finger spread, double tap, wave left and wave right. Importantly, MYO can only sample each channel at a rate of 200 Hz, which is five to ten times slower than the typical sampling frequencies used for sEMG (see the start of the Requirements subsection for more details). The practicality, ease of use and reasonable price tag of Thalmic Labs' product has prompted many groups to evaluate it and try to integrate it in their research, and in spite of its age and it not being produced anymore, it still appears regularly in scientific literature in 2025.

For example Mendez et al [12] have compared MYO with a conventional sEMG setup (6 cable electrodes, 2 kHz sampling rate) for classification of nine hand positions. Despite a 10 times slower sampling frequency the MYO armband produced good results, although bested by the conventional setup (mean classification errors of 5.82 ± 3.63% and 9.86 ± 8.05% respectively).
Tepe & Erdim [13] reached a 96% accuracy in identifying 6 finger gestures with artificial neural networks, using as input the EMG and gyroscopic signals of MYO.
MYO has also been used as a control interface in the context of robotic hand prostheses in the Modular Prosthetic Limb project by John Hopkins University, either as a training implement [13, p.3] or directly for prosthesis control [15].

In different application fields, Indraccolo & De Paolis [16] prototyped an augmented reality system allowing surgeons in the operating room to visualize the patient's organs and medical information easily and hands-free through the use of the MYO armband, Yao [17] used the product to monitor arm movement of stroke rehabilitation patients while Zsoldos et al [18] developed a remote control application for a robotic manipulator arm by combining MYO with deep learning.

As mentioned before, the MYO armband is not in retail anymore. Thalmic Labs sold their patents to CTRL-Labs, which have used them to develop the CTRL-Kit armband. CTRL-Labs having been shortly thereafter bought by Meta (Facebook's parent company) and the product discontinued, there is very little information available about the CTRL-Kit [19] . Only one research article using it was found, briefly mentioning that it was capable of sampling 16 EMG channels separately at 2 kHz each [17, p.3].

Two companies have recently put out new sEMG solutions on the market : the soberly named EMG Bracelet by Synchroni [21] and the uMyo by Ultimate Robotics (in two completely different price ranges, 3800$ and 50$ respectively). Synchroni's solution proposes 8 EMG sensors with variable resolution and sampling frequency (8-bit at 1000hz or 12-bit at 500hz), as well as a 9-axis IMU and Bluetooth Low-Energy (BLE) communication. As for uMyo, their project is open-source but no details about its capabilities could be found except that it possesses 4 EMG channels, a 6-axis IMU and BLE communication [22].

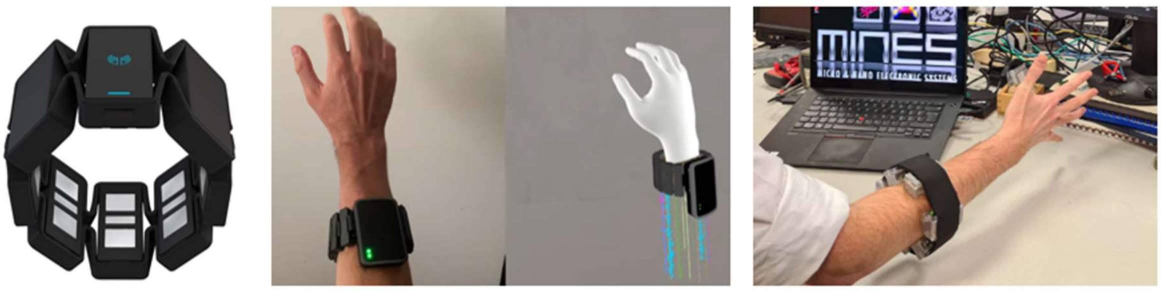

Figure 1 : (left to right) MYO, CTRL-kit & Mongardi's et al EMG bracelets [23], [24],[9]

Design Process

The design process for a complex PCB is often iterative : after the requirements are established and components chosen, a first layout is drawn then reviewed by other PCB designers to point out the inevitable mistakes. Especially in an environment like N-Pulse, where requirements and sub-systems might change dynamically along the semester, two to four reviews might be necessary before having a ready-to-manufacture product. As the PCB is ordered, assembled and tested it often so happens that the first prototype functions partially or not all. In this case, the bugs must be pinpointed, corrected and the new design reviewed again: the design process starts over for a corrected version. In the case of this semester project it was clear from the start that we would not have had the time to redesign a second version of the Signal Processing board after testing of the first one, so the goal was to design the first one carefully enough as to have at least a partially functioning prototype at the end of the project.

To achieve this goal, the first step to successfully develop a new product is to establish a meaningful list of requirements that need to be fulfilled.

Requirements

The previous semester project laid out some initial requirements for the board which were refined in the first weeks of this project.

Essentially, the Signal Processing board has to satisfy the following minimum conditions :

- A **12-bit Analog-Digital-Converter** (ADC) capable of handling **16 channels** at a sampling rate **above 100 kHz**
- A **microcontroller unit** (MCU) **with FLASH size 100 kBytes, RAM size 450 kBytes** and **clock frequency 88 MH**z
- **UART communication** to communicate with external PCBs
- An **USB-C interface** to follow industry standardization
- Wireless communication over **Bluetooth Low-Energy** (BLE)
- **Three power-supply options** : by battery, through the USB port or directly by another board*
- Can **power the signal acquisition modules**** (only one output pin needed: the modules power each other in a daisy chain topology)

*The battery in question would be a 2S battery such as [25], presenting a voltage between 8.4V and 7V depending on charge level. The USB provides 2.5W at 5V, and so would the power board of N-Pulse's prosthetic arm.

**Since the custom signal acquisition modules are not very precise and are still in the process of amelioration, N-Pulse has also acquired BioAMP EXG PILL [26] commercial EMG boards as backup. The Signal Processing board should be able to accommodate both, i.e. provide 1V8 for the custom module and 5V for the BioAmp EXG PILL.

The first two of these requirements are the most crucial. Indeed to fulfill the board's goal, the ADC must be able to sample the EMG signals through with enough precision and speed to extract high quality features, while the MCU needs enough memory size and clock frequency to store and run in real-time (>300ms delay) an ML algorithm using these features to classify hand gestures.

The way the requirements pertaining to these two essential components are obtained is detailed in the following.

ADC :

The ADC's role is to sample a time-continuous signal (the analog signal provided by the acquisition boards) and convert it to a time discrete signal which is understandable and useable by the MCU for further processing.

Nyquist's sampling theorem [27] states that to accurately reconstruct the entire information contained in a time-continuous signal, the sampling frequency must be more than twice the highest frequency of the time-continuous signal.

$$f_s > 2f_{max}$$

Knowing that the bandwidth of an EMG signal is 5 Hz to 500 Hz, we need to sample each EMG signal at a rate at least greater than 1000 Hz. In fact it is desirable to sample at 3 or 4 times the bandwidth of the signal (1500 – 2000 Hz) because the sampling theorem assumes some ideal properties that are not reflected in real systems. [28]
Since the board has 16 EMG channels, the sampling rate needed to sample all of channels accurately should be at a strict minimum 16 * 1000 Hz = 16 kHz, but preferably double that at 32 kHz. Considering that the ADC needs to switch to the next channel after each sample, which takes some time, a safety factor of 3 is a good idea. Thus we obtain a minimum sampling rate of 100 kHz. A larger sampling rate is probably desirable.

The resolution of an ADC over a certain voltage in function of its range and the number of bits is given by:

$$resolution = \frac{range}{2^{n_{bits}}}$$

Through discussions with N-Pulse team leaders it was decided that 12-bits would be precise enough, corresponding to a resolution of ~1.22mV/div for a 5V range (e.g. signal range provided by the BioAMP module) and 0.44mV/div for an 1.8V range (provided by N-Pulse's module).

To calculate which requirements the MCU needs to fulfill, we need to have some idea of what algorithm will be used. N-Pulse's direction indicated that they would like to use neural networks (NN) optimized for low-power portable devices, such as the one proposed in "A Hardware-Efficient EMG Decoder with an Attractor-based Neural Network for Next-Generation Hand Prostheses" by Kalbasi et al [29].
The authors propose a compact NN with less than 7000 parameters which still manages a high accuracy of 80.6 % when decoding coarse and fine hand and finger movements. Assuming that the parameters are stored in the 'double' data type on 8 bytes (worst case scenario in the terms of memory usage, 'float' data type i.e. 4 bytes is more common) this amounts to 7000*8 = 56 kB of FLASH memory necessary for the model.
The authors also mention that they first sample at 2400 Hz across 64 channels. In our case the signal Processing Board has 16 EMG channels and according to our real-time requirement we might only keep 0.3 second of EMG data.
This gives us 16*2400*0.3*8 = 92,16 kBytes of RAM storage to store the raw EMG data buffer.
The input stream is then downsampled to 100 Hz and "[…]segmented into 200 ms data blocks with

190 ms overlap between windows, which is equal to 20 data samples per block for predicting each output.”[29, p. 534]. Segmented and repeated 20 times in this way, the 200ms block (downsampled to 100 Hz -> 20 datapoints) will take up nb_block*nb_datapoints*nb_channels*datasize = 20*20*16*8 = 51,2 kBytes of RAM storage. Together this amount to ~ 150 kBytes of RAM storage. Accounting for other operations which might need to be stored temporarily, we will take a safety factor of 3 and require a RAM capacity of 450 kBytes.

Finally we want to estimate the desired clock frequency to run this algorithm. To this end we will roughly estimate the number of operations necessary for one estimation output, based on the model architecture.

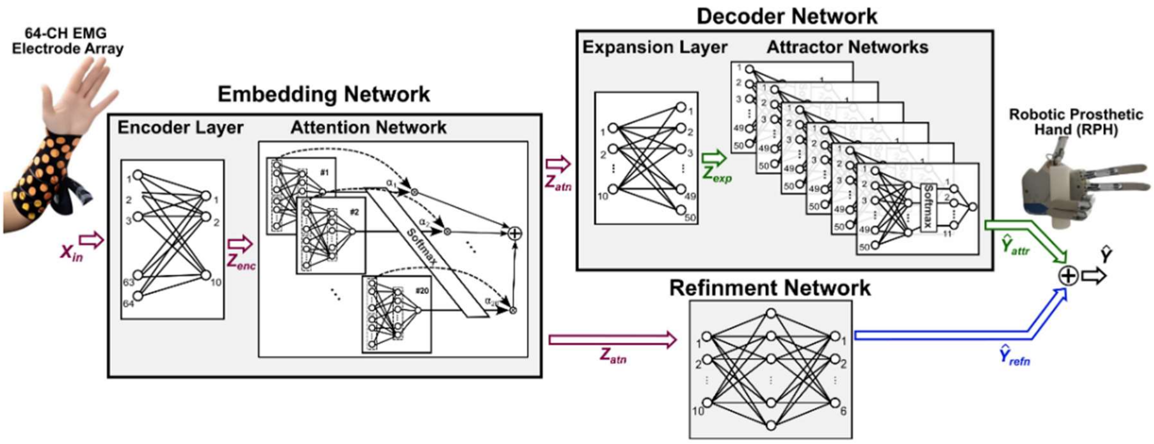

Figure 2 : Kalbasi et al's Artificial Neural Network architecture [23, p.2]

A **single-layer perceptron** (SLP) such as the one used in the encoder, expansion or attractor layers is simply a weighted sum, so for N inputs and M outputs it needs to add and multiply (N*M) times, which is done by a **Multiply-Accumulate** operation (**MAC**). In the following we will denote it as an N-M SLP, which requires N*M MAC operations..
A **two-layer perceptron** (2LP) such as the ones used for the attention or attractor networks is equivalent to two SLPs in a row. As such, an N-M-P 2LP (N inputs, middle-layer size M, P outputs) requires N*M + M*P MACs.

The model starts with the 64-10 encoder SLP (=640 MACs). But it has to be repeated for each of the 20 timesteps used in the 20-block segmentation technique described above, which totals to 12800 MACs.
It then goes into the 2LP attention network composed of 20 different 2LPs which each have two 10 dimensional inputs, one middle layer of unknown size (we will assume 10) and outputs a single 1D scalar. Thus we have twenty 20-10-1 2LPs for a total of 20(20*10 + 10*1) = 4200 MACs.
Then we pass through the 10-50 expansion SLP (500 MACs) and into the attractor networks : six 50-11-11 2LPs (total of 4026 MACs). Finally there is also the refinement network with 10 inputs, unknown middle layer size (assumed 20) and 20 outputs, which results in in 10-20-6 2LP requiring 320 MACs.
Thus a very rough estimate of the total number of multiply-accumulate operations for one prediction output is 12800+4200+500+4026+320 ≈ 22 000 MACs.
Considering that some steps have been skipped, the fact that the MCU will need to carry out other

instructions simultaneously (such as communicating with the ADC to obtain the values in the first place) and the approximate nature of this estimation, taking a safety factor of 2 is a good idea, bringing the total to **44 000 MACs**.
Knowing that one MAC can usually be processed in two clock cycles [30] and that to fulfill our real-time requirement we want to have a very small inference time, let's say t_{inf} =1ms, we can calculate the necessary clock frequency as follows : $f = \frac{2*MACs}{t_{inf}} = 88\ MHz.$

In Figure 3, the functionalities of the board have been organized in a block diagram for easy visualization.

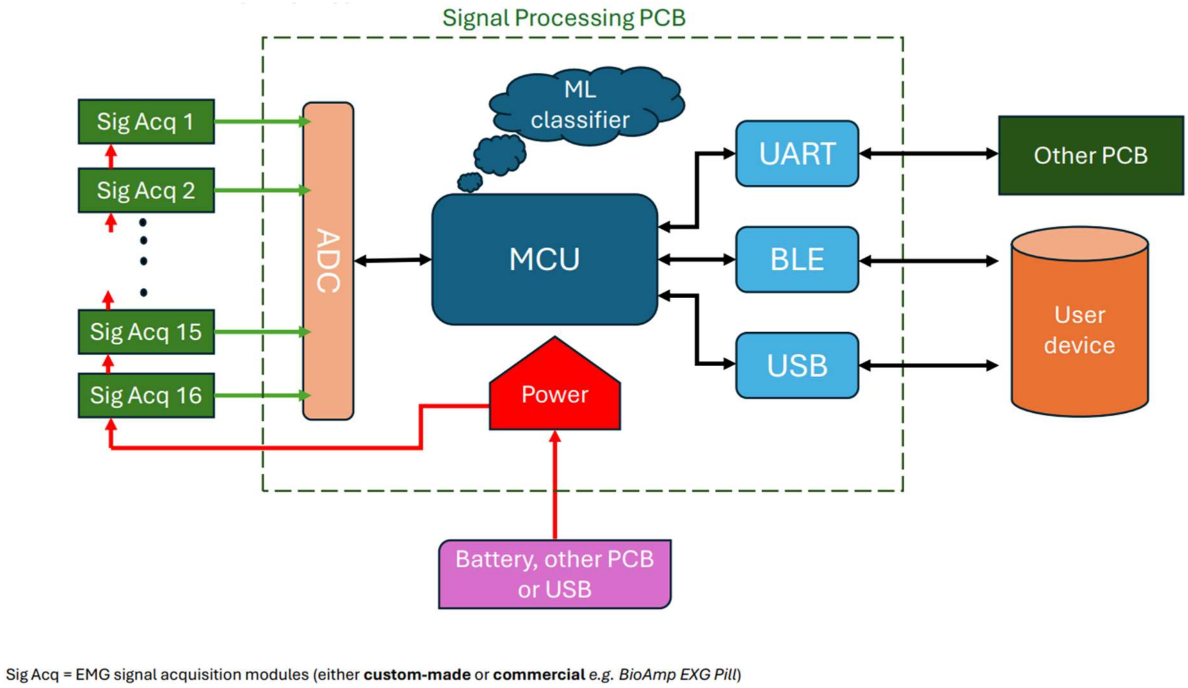

Figure 3 : Block diagram of the board's functionalities

Design choice : Board as prototype

Given that it is my first time designing a PCB and that no other member of N-Pulse had experience designing a board of the same complexity as the Signal Processing board, it was suggested by Professor Schmid that we develop a board with the explicit goal of being a prototype and not a compact and optimized product.

In consequence different features were chosen to try different solutions together and evaluate which one works better. This allows us to keep some flexibility to get around predictable mistakes and allow visibility into the inner workings of the board to debug mistakes more easily.

Test points

Test points are the first debugging feature : they are exposed copper pads or rings where a multimeter or oscilloscope probe can be applied to measure voltages or observe signals. They are disseminated on important points of the PCB to allow measurement of signals of particular interest for the operation of the board. For example test points are available to measure each of the voltages used for power delivery (5V, 3V3, 1V8, GND), at the output of some components (such as the operational amplifier which buffers the EMG channels) or on UART and SPI communication lines.

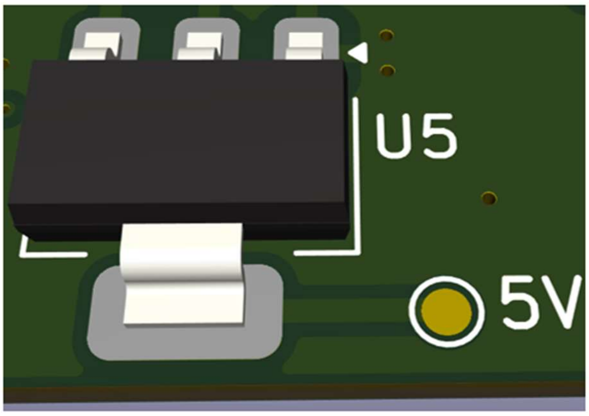

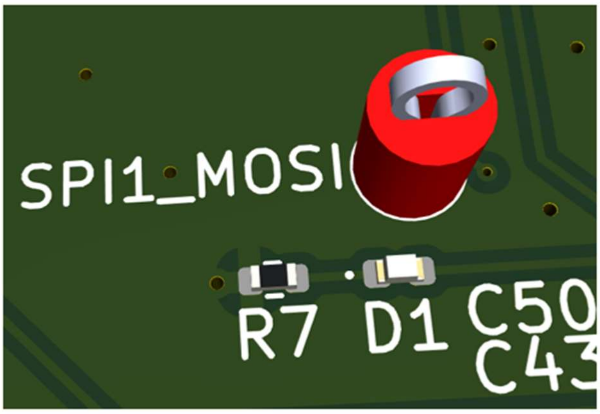

Figure 4 (left to right) exposed pad on 5V output of LDO, 5260 ring exposing an SPI communication line (3D renders in KiCAD)

Multiple Antennas

The second prototyping feature is the use of multiple antennas. Without experience in such a complex domain as radio frequency (RF) antenna design, even choosing what type of antenna is appropriate for an application becomes arduous. In consequence it was decided to install the thre ain types of antennas available for PCBs at the same time which will enable us to compare their performance and decide which one to keep for the next version of the Signal Processing board.
An added bonus of redundancy is that even if one of them does not work because of design mistakes, there is a backup and second backup antenna, ensuring a good chance that at least one will work.
Of course using multiple antennas at the same time could cause significant interference, so an RF-capable switch is used to activate one at a time.

The three antenna types in question are :

1. **External antenna** : connected to the board via a male U.FL connector.
2. **Ceramic chip antenna** : premade surface mount device (SMD) component soldered onto the board like all other standard SMD components.

3. **Trace antenna** : etched as a simple copper trace directly into the PCB

Figure 5 : (from left to right) externa [31]l, ceramic chip [32] and trace antennas

Jumpers

Finally, pin header jumpers and solder bridge jumpers were used to leave flexibility in some parts of the circuit whose correct behavior was not entirely certain. They provide a simple and somewhat reversible hardware way to manually (dis)connect or reroute the copper traces carrying the electric signals.

An example of this is the solder bridge jumper JP2 which connects the VDD11 and VDDRFPA pins of the MCU. It was difficult to judge from the MCU's datasheet if these two parts of the power circuit should be connected. After looking at a reference PCB using a similar (but not exactly the same) MCU it was decided to leave them unconnected, but an unconnected solder bridge jumper was added between them as a backup option. In case we discover that this connection is needed, a small solder drop can easily be dropped on JP2 to close off the circuit and connect the pins.

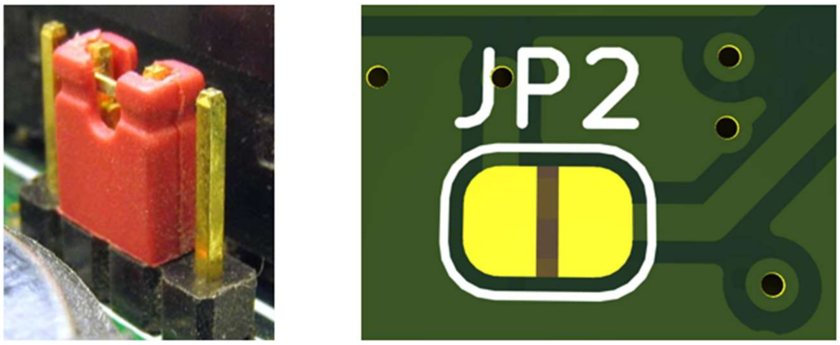

Figure 6 : Pin header jumper (left)[33] and unconnected solder bridge jumper (right)

Product

After two review rounds the first prototype version of the Signal Processing Board, nicknamed “EMG Live Estimation and Analysis” (ELEA) was sent off to JLCPCB [34] for manufacturing.

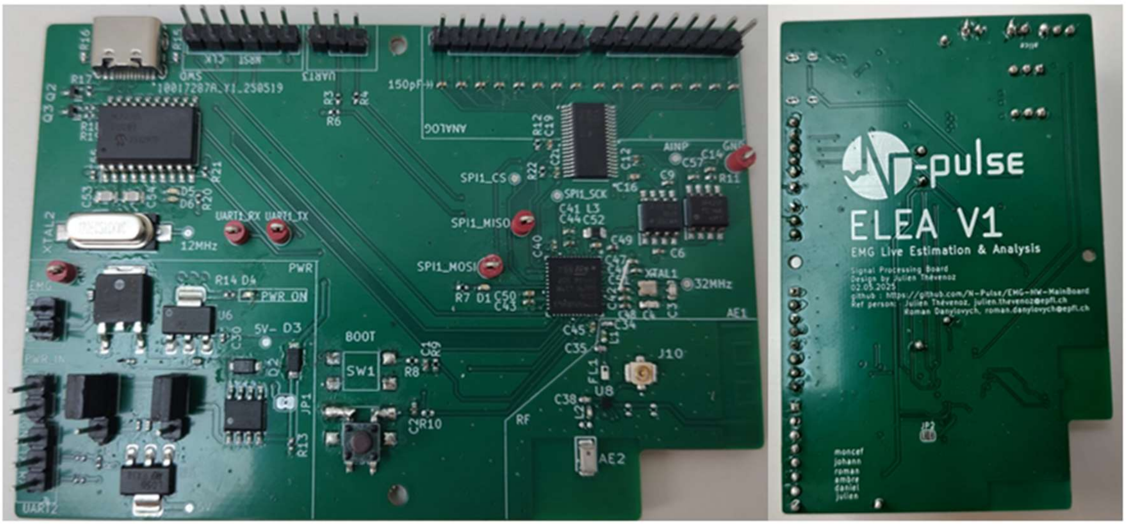

Figure 7: Front and back of ELEA board

The board itself is roughly 10mm x 6mm and 1.2mm thick. It is a four-layer board arranged in a typical stack-up (top and bottom layers serve to route signals, both middle layers serve as power planes) and follows one of the manufacturer’s standard empilement (JLC041211-7628 [35]):

1. The top layer carries most signals (radio frequency, digital, analog,…),
2. the second layer is a ground plane,
3. the third layer is a 3V3 plane
4. the bottom layers carries a the remaining digital signals which could not be routed on the top.

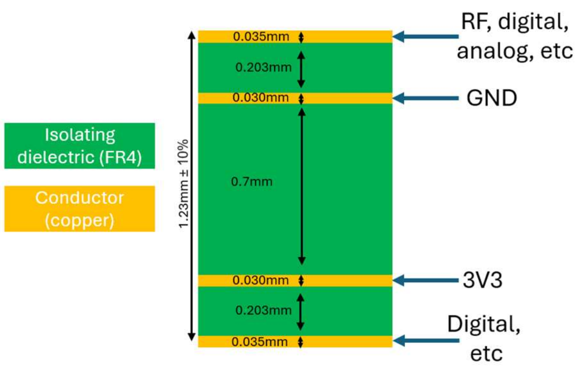

Figure 8 : Vertical layer order and dimensions of ELEA

Block diagram

For a clear understanding of the system, a block diagram detailing all the important functional blocks was created.

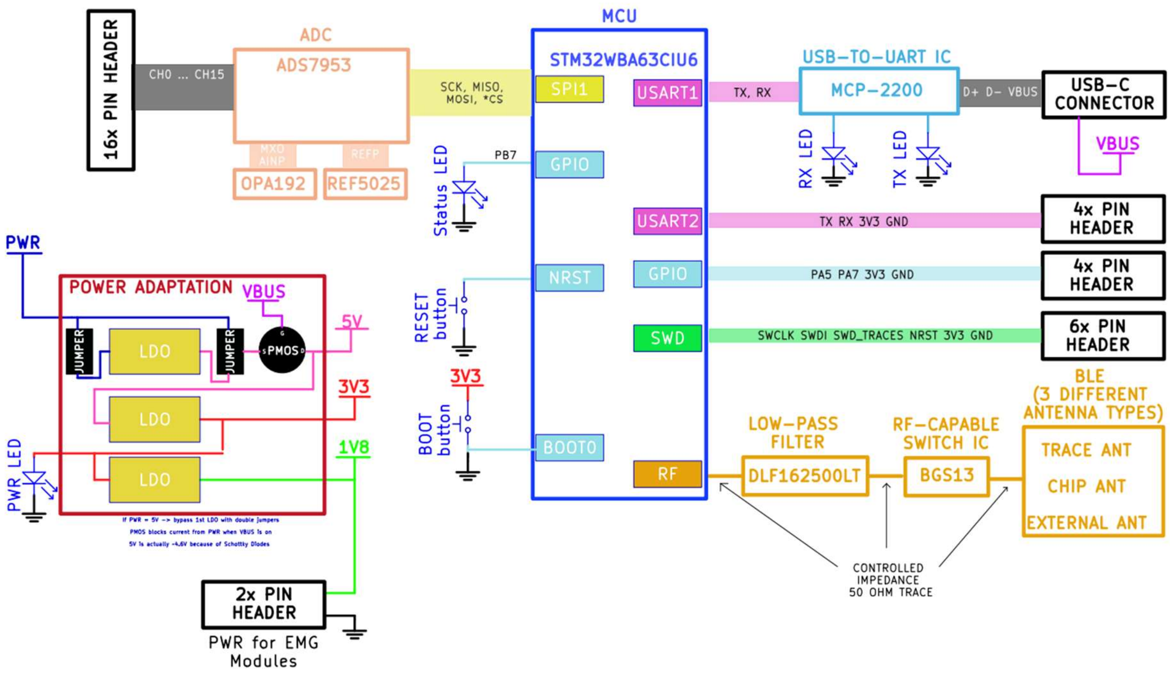

Figure 9 : Block diagram of ELEA 1st prototype

In the middle, the MCU is the brain of the whole board. It communicates with the ADC through SPI protocol to set sampling parameters and obtain the recorded values, and sends its results to other devices through USB-C (first by UART which is then translated into USB protocol by the MCP-2200), directly through UART or by Bluetooth Low-Energy through one of the antennas. Different LEDs indicate if the board is powered, if the MCU is functioning correctly or if USB-C traffic is occurring.

The Serial-Wire-Debug (SWD) connection provides a practical programming interface for the MCU.

On top of the connectors necessary for the 16 EMG signal acquisition modules, the many pin header connections available on the board allow for varied interaction possibilities with the MCU (through UART, SWD or GPIO pins), useful for debugging.

The power section is displayed in the bottom right corner. It serves to provide the necessary 5V, 3V3 and 1V8 power to the board components and signal acquisition modules. The board can be powered either through the PWR line with a 5V or above voltage, or through the USB-C connector (top right) which when connected feeds into the power section through the VBUS lin.

In-depth presentation

The important aspects and subsystems of the Signal Processing board will be presented. For complete electronic schematics and plane by plane layouts, please refer to the annexes.

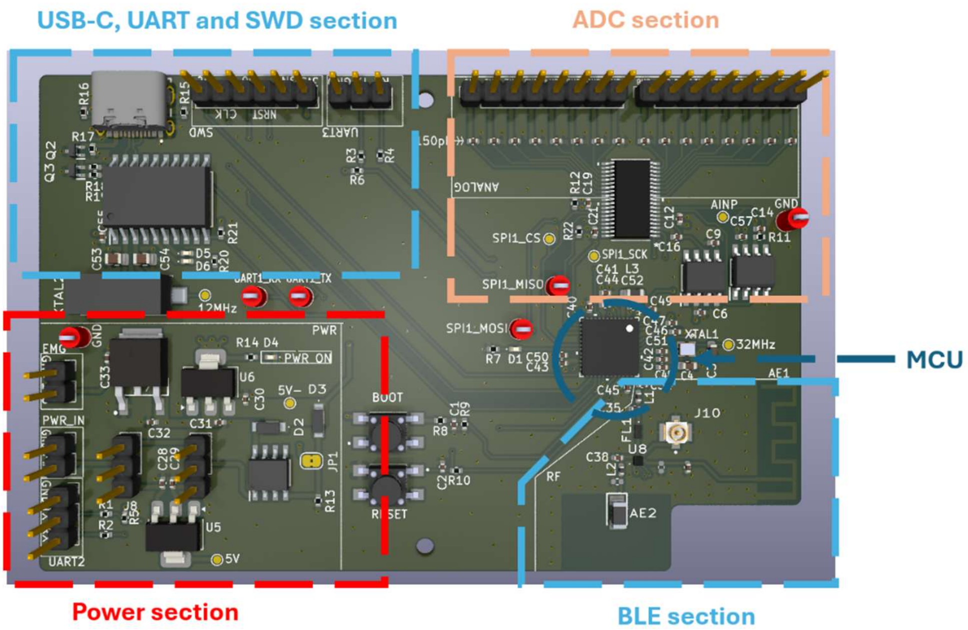

Figure 10 : Important functional blocks of ELEA board (KiCAD 3D render)

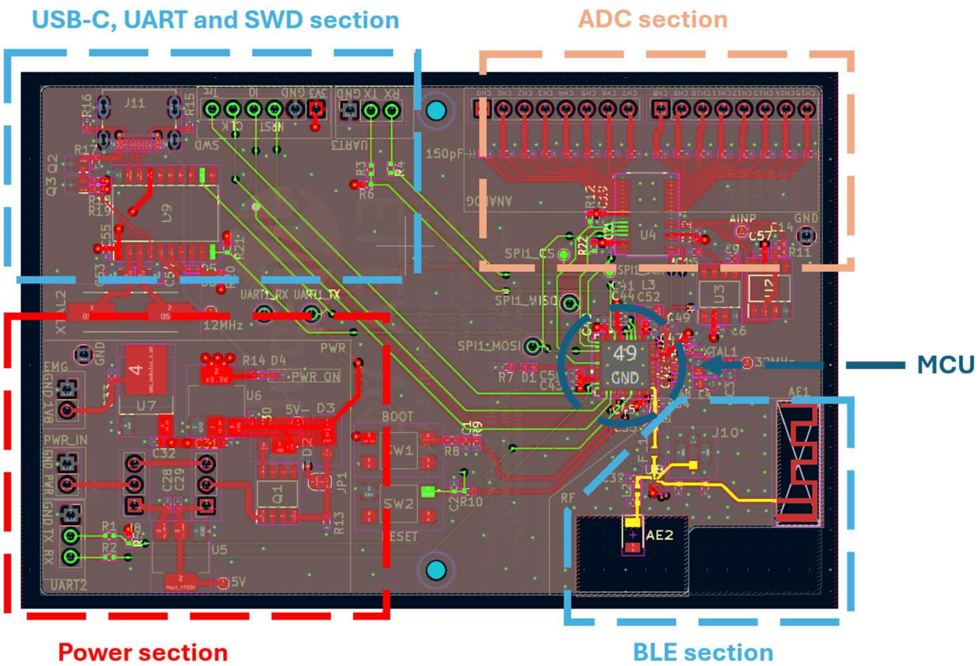

Figure 11 Important functional blocks of ELEA (KiCAD PCB layout)

Power section

The Signal Processing board was designed to have flexibility in its power supply options. In its main application as a part of the EMG Bracelet, it should be powered by a battery or through its USB port. In the eventuality of integrating it directly in N-Pulse's robotic hand prosthesis, the board also has the option of being supplied by an external 5V source such as the prosthesis' dedicated power board. The EMG Bracelet's on-board power supply would be a 2S type battery which possesses a voltage varying from 8.4 to 7.6V depending on charge level.

Most of the components on the board are powered by a voltage of 3.3V (except the OPA192 op-amp), but there is still a need for 5V available on the board in the situation where the signal acquisition modules are the commercial BioAMP EXG PILL modules. When N-Pulse's custom modules are used however, they require a power supply of 1.8V.

In consequence the board possesses three linear-dropout (LDO) regulators in succession to obtain 5V, 3V3 and 1V8 respectively from the battery input. LDOs are less efficient than other types of voltage regulators since they dissipate the extra-power as heat, but they were chosen since they are simple and don't produce additional noise like switching converters.
If the power is not supplied by a battery but by a stable 5V power source, two jumpers around placed before and after the first LDO can be used to bypass it.
In case a USB cable is plugged into the board, a simple circuit (a P-MOS transistor and a pull-up resistor) effectively disconnects the power line (whether connected to battery or external) and draws current only from the USB supply through the VBUS line.

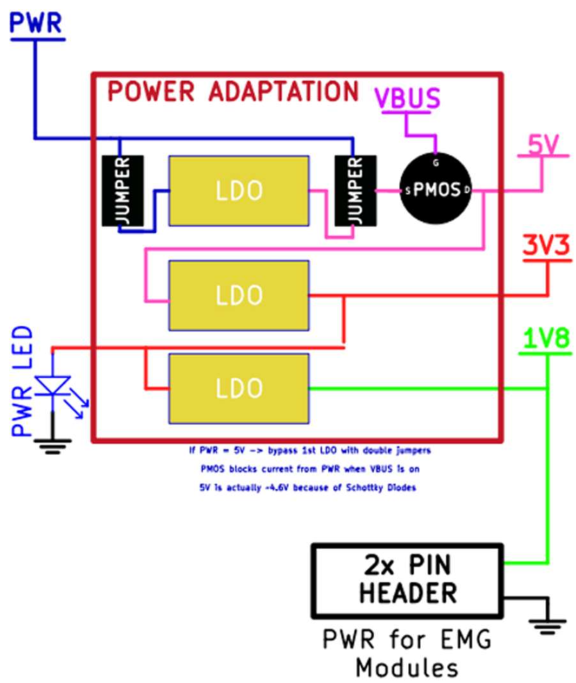

Figure 12 : Diagram of the power section (snippet from Fig 7)

This three stage voltage adaptation scheme is typical of the prototype nature of the ELEA board : it is not ideal at all because it wastes a significant amount of energy and creates a lot of heat, but it offers the flexibility of powering two different types of acquisition modules.

Micro-controller unit

The chosen MCU is an STM32 model WBA63CI which presents the following attributes [36].

Characteristic	Value	Requirement (if applicable)
FLASH memory size	2 Mbytes	100 kBytes
RAM size	512 kBytes	450 kBytes
Clock frequency	100 MHz	88 MHz
RF capability	Bluetooth Low-Energy 5.0 (BLE)	N/A
Communication interfaces	UART, SPI, I2C	UART

Other members of N-Pulse were already developing PCBs with STM32 products and using the same family of MCUs across the association makes knowledge transfer and development easier. The WBA63CI was the model with the highest combination of FLASH and RAM and the integrated ability to drive an RF antenna. An alternative idea could have been to use an exterior module to take care of the BLE communication (such as the ESP32-S3 Wroom [37]) but it was decided against on the grounds that more components entail more space, energy consumption and complexity.
Unfortunately the WBA63 does not integrate native USB communication, so it is handled separately as explained further below.

Analog-Digital Converter

The selected ADC is an ADS7953SBDBT by Texas Instruments which presents the following characteristics [38].

Characteristic	Value	Requirement (if applicable)
Resolution	12 bits	12 bits
Input channels	16	16
Sampling frequency	1 MHz	100 kHz
Communication interface	SPI	N/A

A stable, high precision voltage regulator IC (REF5025[39]) provides the ADC with a stable 2.5V reference voltage to accurately take measures. The ADS7953 is software configurable to sample over a range of 1x Vref or 2x Vref, which makes a 2.5V source ideal for our needs, since we can select the 1x range for N-Pulse's custom EMG acquisition modules (output range 0 to 1.8V) and 2x range for the BioAmp module (output range 0 to 5V).

Although a sampling rate of 1 MHz sounds impressive, it doesn't tell the whole story. Indeed the internal 16-to-1 multiplexer of the ADS7953 lengthens the settling time (delay needed by the ADC to sample correctly) between each sampling action proportionally to the source impedance presented to each channel (i.e. the output impedance of the signal acquisition module) is large. In the datasheet, TI provides graphs of the sampling rate in function of the source impedance and solutions to mitigate the decrease in sampling rate.

I tried to measure the output impedance of N-Pulse's custom modules using a simple load resistance and voltmeter setup, but obtained inconclusive results. Indeed to validate the results, the measurement was conducted with different resistors of values ranging from 100 Ohm to 1 MOhm, which produced output impedance values ranging from 23 Ohm to almost 100 kOhm. No value of output impedance could be determined.

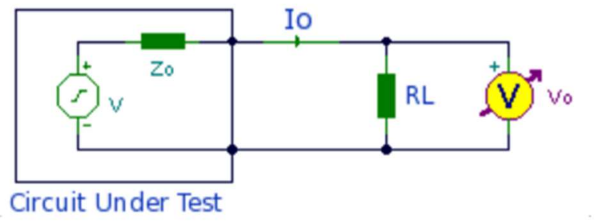

$$Z_o = R_L * \left(\frac{V - V_o}{V_o}\right)$$

Figure 13 : Output impedance (Zo) measuring method (V = open-circuit voltage, Vo = loaded circuit voltage, RL = load resistance). Image credit [34]

In absence of a specific value to optimize for, effort was made to accommodate for a worst case scenario and thus all possible precautions listed in the datasheet were followed. In particular, additional components such as capacitors in parallel to each input channel and an operational amplifier OPA192 [40] acting as a buffer between the ADC’s internal multiplexer (MXO) and analog input (AINP) were added to mitigate sampling rate loss. See the following diagram.

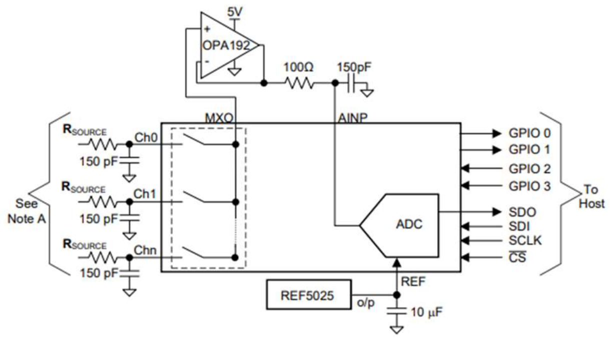

Figure 14 : Application diagram for the ADS7953 buffered with an OPA192 [38, p. 50]

This setup allows for the slowest decrease in sampling rate for the 12-bit version of this ADC, decrease which is characterized in Figure 10. We can see that even for an output impedance of 10 kOhms, we maintain the required 100 kHz sampling rate.

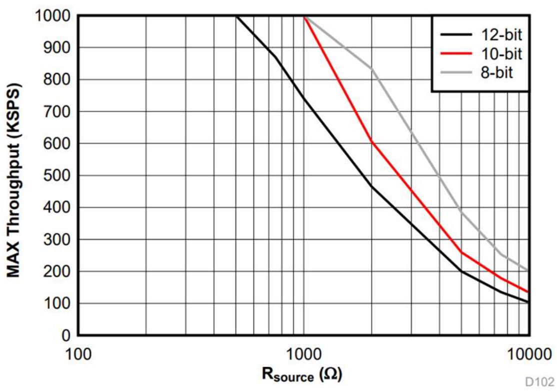

Figure 15 : Sampling rate (kilo-samples-per-second i.e. kHz) in function of source impedance [15, p.51]

USB-C port and communication

Integrating an USB-C port to the board is useful since USB-C is one of the most commonly used connectors: allowing easy powering, communication and programming of the board/bracelet. The USB-C port is capable of providing a current of 0.5 Amps at 5V through its VBUS line.

Since the MCU does not have USB On-The-Go (integrated USB protocol capability), the board needs an IC which translates USB communication coming from the USB-C port to a protocol that the MCU can understand. To this end the MCP-2200 USB-to-UART converter by Microchip[41] was chosen, since UART is an easy and common protocol. The MCP-2200 implements an older version the communication protocol called USB 1.1 or USB Full-Speed which permits a transfer rate of 12 Mbit/s (=1.5 MB/s).
Although significantly slower than modern USB protocols, this speed was judged to be amply sufficient for our application. Indeed even if we wanted to transfer the entire raw EMG data buffer, and assuming sampling each of the 16 channels at a high rate of 2400 Hz (as in [29]) as a float datatype (4 Bytes), the data would only represent 2400*16*4 = 153,6 kB of data per second, i.e. one tenth of the USB Full-Speed's transfer speed.

Bluetooth Low-Energy RF design

The STM32 WBA6 family is capable of different radio communication protocols in the 2.4 GHz frequency range and has the internal circuitry to drive an antenna through its special RF pin.

Figure 2. 2.4 GHz RADIO block diagram

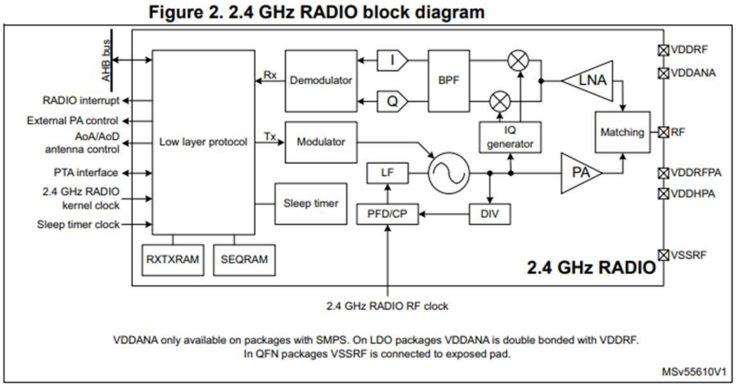

Figure 16 : STM32WBA63 RF circuitry [13,p.28]

Of special interest for us is the Bluetooth Low Energy (BLE) protocol, which is a short range wireless technology focused on Internet-of-Things (IoT) applications. Using short information transfers and falling back to sleep mode quickly between communications allows it to consume little energy, making it ideal for battery-powered and low-power devices [42].

<u>Impedance matching</u>

To allow the radio signal to travel intactly to the antenna it must be carried along a medium whose impedance is constant as to avoid impedance discontinuities for electric waves at high frequencies which cause undesirable phenomena such as reflection, standing waves and suboptimal power transfer[43].
As a consequence, most RF parts and circuits are designed to function for a standard impedance value of 50 Ohm, and components and transmission lines are adapted to obtain this value in a process called **impedance matching**.

In particular the wire or, in the case of a PCB, the copper trace linking the different parts of the circuit must be specifically manufactured to obey this 50 Ohm value. Parameters such as trace width, height and distance to ground plane and other conductive elements must be considered to create an impedance controlled trace.
For our use, a **coplanar waveguide topology** was selected and the necessary parameters were calculated using the manufacturer's online impedance calculator (and explicitly validated through email by the manufacturer's engineers). The dielectric height h being given by the board stack-up (0.203mm), the parameters W and S were found to be 0.36mm and 0.3208mm respectively.

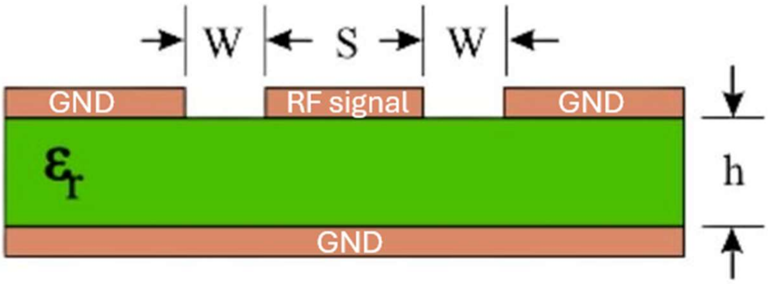

Figure 17 : Coplanar Waveguide topology (original image from)

The RF pin of the MCU itself isn't designed for 50 Ohm and must in consequence be matched to the standard value using a inductors and capacitors arranged in a **Pi-type impedance matching network**.

The values for the pi-matching network were taken from an STMicroelectronics application note [44, p. 14] for the WB55 family of MCUs.

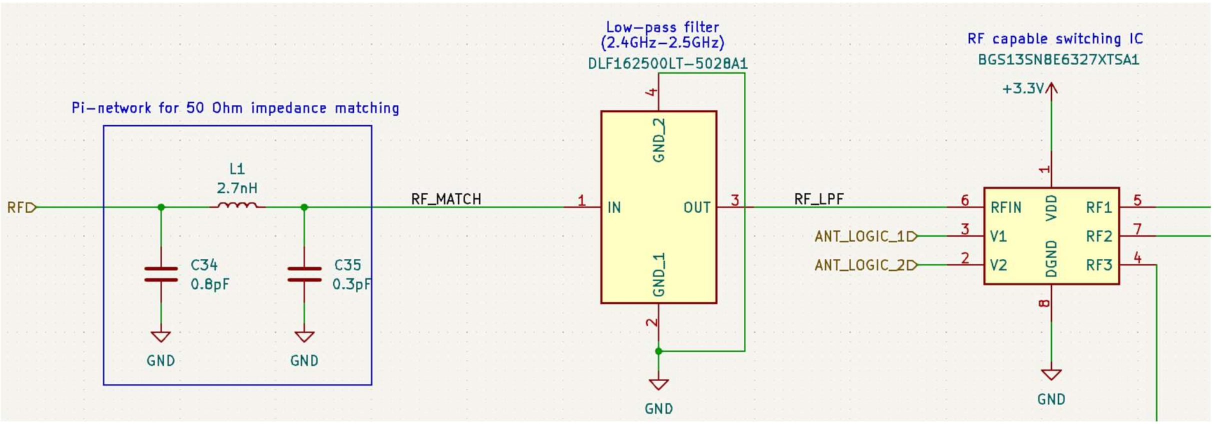

Figure 18 : Pre-antenna RF circuitry (KiCAD schematic editor)

After asking a question on the ST Community support forum [45], ST engineers provided the complex impedance for the specific WBA63 model of the signal processing board, which allowed me to calculate the correct values of the matching network. Since the EMG Bracelet is only expected to communicate with devices in a range of a couple meters we can assume a 5dBm transmission power will be enough, corresponding to a complex impedance $Z_{max} = 22.7 - j9.3$ Ohms. With this knowledge (and assuming a Q factor of 5) I can use an online pi-matching calculator such as [46] to find the desired values.

Inductance	Source capacitance	Load capacitance
1.09 nH	6.63 pF	7.92 pF

They are quite different to the values of the application note. Unfortunately, when the ST engineer's answer was published it was too late to change the components since the order had already been made and the components arrived.

After the matching network, the controlled impedance trace passes through a low-pass filter component and into a switch IC [47]capable of handling RF frequencies without distorting the signal. This IC then allows to select which antenna is used.

<u>Three Antennas</u>

As mentioned earlier, three antenna types are installed on the board for redundancy and testing.

The external antenna, an FXUB63.07.0150C by Taoglas[48], is the most reliable antenna but also the most expensive and cumbersome one by far. (NB this specific antenna just happened to be left over from another N-Pulse project, it is 2.4 GHz compatible but not specifically optimized for that frequency).

The ceramic chip antenna by Abracon [49] is a good compromise, being compact and affordable but needing more care in the design process.

Finally, the trace antenna is the cheapest and most compact antenna by nature since it is not an additional component but simply a copper trace carved into the PCB material. It is also the most finnicky to implement, requiring extreme care in the selection of all different aspects of the antenna (dimensions, shape, board thickness). The one used on the ELEA board was modeled according to a Texas Instrument application note [50] whose layout is available by default in the KiCAD PCB editor software. The stack-up of ELEA was chosen to resemble the one used by a TI dongle [51] implementing the antenna in question, but imitating it exactly would have been too expensive to manufacture. Since trace antennas are so sensitive to even small changes in any of the parameters that they were designed for, I expect that it will most probably not function. Since it costs almost nothing however, it was still kept in the design as a "what-if".

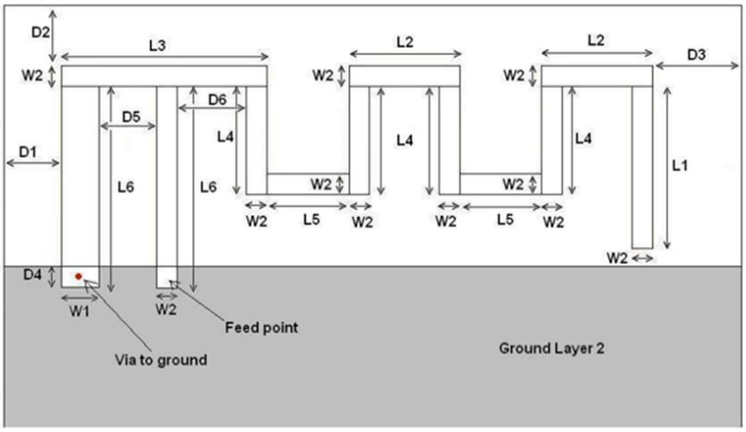

L1	3.94 mm
L2	2.70 mm
L3	5.00 mm
L4	2.64 mm
L5	2.00 mm
L6	4.90 mm
W1	0.90 mm
W2	0.50 mm
D1	0.50 mm
D2	0.30 mm
D3	0.30 mm
D4	0.50 mm
D5	1.40mm
D6	1.70 mm

Figure 19 : Small size 2.4 GHz antenna from Texas Instruments application note AN043 [50]

Testing

Due to diverse delays in the ordering and delivery of the PCB, the Signal Processing board was only able to be assembled four days before the project report was due, meaning there was very little to

time to test and debug the board.
In consequence, a thorough testing program was devised and carried out as far as possible. The steps undertaken and results obtained are described in the following, and the rest of the program will be finished after the end of the academic part of the project.

The measures for voltages and signals were done using an HMP2030 programmable power supply, a Fluke 115 digital multimeter and an RTB2004 digital oscilloscope. An ST-Link V3MINIE probe was used to communicate and program the MCU.

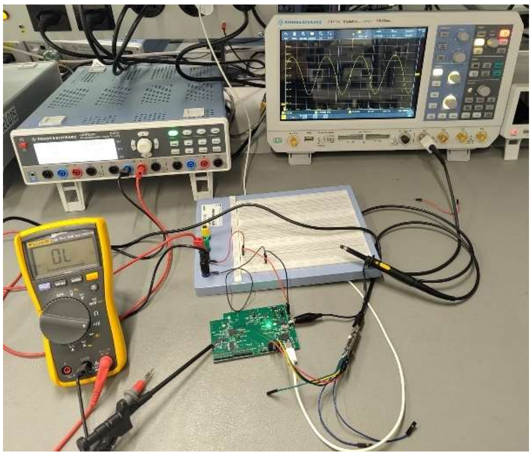

Figure 20 : Test setup

Table 1 : Testing procedure

--- NO POWER ---		
#	Step	Remark
1	Visual Inspection	Some LEDs wired in the wrong direction -> desolder and resolder. Apart from that OK
2	Test for short circuits between power stages	OK
--set jumpers to bypass 5V LDO -- --- POWER WITH **5V** CURRENT-LIMITED LAB POWER SUPPLY ---		
3	Power-on inspection : PWR LED on ? smoke, smell, excessive heating ?	OK
4	Verify voltages on relevant test points (5V, 3V3, 1V8, GND, …) and current draw from lab supply	Mostly OK *1 Draw : 20 mA
--set jumpers to include 5V LDO -- --- POWER WITH **8V** CURRENT-LIMITED LAB POWER SUPPLY ---		
5	Repeat steps 3 and 4	Same results Draw : 25mA
--- power through USB port only ---		
6	Repeat steps 3 & 4	Same results *2 Draw : N/A
--- power through USB port AND lab supply simultaneously ---		
7	Verify that current draw from lab supply drops to 0	OK *3
--- power through whichever preferred method ---		
8	Verify communication with MCU through ST-Link	At first non-functioning, in depth inspection revealed & solved problem on the MCU's N-Reset pin *4 *5

9	Flash blink code over ST-Link	OK *6
10	Verify oscillator frequencies (32MHz & 12 MHz)	31.986 MHz and 12.001 MHz : OK
Preliminary verification that components are working		
11	Try PC-MCU communication over UART	Transmit & receive with interrupts over UART2 on serial terminal of PC using FTDI223 interface : OK
12	Use MCP configuration utility software to see if MCP2200 chip works	Software recognizes MCP2200 when USB cable plugged in PC : OK
13	Verify basic function of SPI (check NCS, SCK & MOSI signals with oscilloscope)	OK
14	Try basic MCU-ADC communication over SPI (read/write a register)	
15	Verify functionality of RF switch IC (check if changing V1/V2 of IC modifies which output channel is selected)	
16	Verify basic function of 3 RF antennas (send any signal through the antenna and try to detect it with an RF receiver)	
Implementing the proper code to use different components		
17	Implement MCP2200 communication protocol -> PC-MCU communication over USB port	
18	Implement ADC communication protocol -> try to read a voltage from an input channel (send it over UART ?)	
19	Transmit meaningful signal over RF	
20	Receive and decode signal over RF	

Table 2 : Additional comments

*1	All voltage points were as expected but the clock signal on MCU's 32MHz external crystal test point could not be detected. (Explanation found in *5)
*2	An oscillation at the correct frequency was measured on the MCP2200's 12 MHz crystal test point (it was not there before because the MCP2200 is not activated unless VBUS is high)
*3	*jumpers in 5V-LDO bypass configuration* 5V (lab supply) without USB connected : current draw from lab supply= 22 mA 5V with USB : current draw = 0 mA *jumpers in 5V-LDO connected configuration* 8V without USB : current draw = 27 mA 8V with USB : current draw = 5mA Even though the PMOS circuit doesn't completely shut off current draw from the battery circuit (8V case), we can conclude that the flexible design of the power section to cater to three different types of power sources is a success.
*4	NRST and BOOT0 buttons were discovered to have been soldered the wrong way around, permanently shorting the path that should be button-activated. This led the NRST pin to be always pulled down to GND, stalling the MCU in reset mode. Desoldering of both buttons and resoldering of the NRST button (BOOT0 being not critical) fixed this issue and allowed communication with the MCU.
*5	In the debug process, another hardware error was discovered : the VDDRF pin (which powers the RF circuitry and crucially the HSE crystal) had not been connected to 3V3 on the

	PCB. As a quick fix, a small wire was pulled between C51 (decoupling capacitor of VDDRF) and C47 (decoupling cap of VDD pin), which allowed VDDRF and thus the external crystal to be powered. A correct 32MHz oscillation was then observed on the HSE test point.
*6	An error systematically occurred in the function “PeriphCommonClock_Config();” of main.c. The HAL_error occured line 495 of stm32wbaxx_hal_rcc_ex.c : if (__HAL_RCC_GET_RADIOSLPTIM_SOURCE() != PeriphClkInit->RadioSlpTimClockSelection) { return HAL_ERROR; } Considering time was pressing and that the Peripherals Clock only seems to concern some radio setting, the line in main.c was simply commented out which solved the error. It will stay like for further tests unless explicitly stated. This error should be investigated at a later time.

Mistakes & Lessons learned

An obvious yet important lesson learned in the development of this first PCB is that, unless there is an excellent reason for it, complicated features should not be designed by ourselves to spare time and prevent potential mistakes making the hardware inoperable.
For example the design RF hardware is such a complex and involved field that it required a huge amount of hours, yet has a high risk of failure. Integrating a module with integrated antenna such as [37] might have allowed the PCB to be ordered and assembled much sooner and thus more thoroughly tested (although adding a second MCU to the board does add some hardware and software complexity which might have offput the time-gain a bit). The same can be said to a lesser extent of the USB-to-UART communication, which could have been solved by selecting an USB On-The-Go capable MCU such as the STM32WBA65, and of even relatively simple features, such as the P-MOSFET circuit serving to cut off the battery line when USB is connected. Despite its simplicity it still took many hours of reflection and simulation to prevent mistakes. An appropriate IC could have done the same thing and enabled the battery to be charged through the USB-port (in the current design, the battery needs to be detached and recharged externally).

A second lesson is to research and use the possibilities of all the available development tools early on. STMicroelectronics provides different excellent software tools such as STM32CubeIDE [52] and STM32CubeProg[53]. I first decided to completely focus on the hardware and neglected to look into these software tools for programming until after the board was ordered, but actually STM32CubeIDE integrates a very handy GUI which allows to configure GPIO pins, communication pins, clocks etc for the specific chosen MCU. The STM32WBA6x is extremely dense and sometimes confusing since it provides information for different models from the same family but it is sometimes hard to understand to which exact model which information applies. As such, using STM32CubeIDE it in the debugging part of the project (when the ELEA board has already been ordered and shipped) made me realize that there was some conflict between functions that I had planned (e.g. SPI1 cannot be used at the same time as SWD or UART2) and even that some functions I had designed for (UART3) were actually missing from my specific model. Fortunately, thanks a combination of luck and redundancy, these mistakes didn’t affect any important subsystem of board. Still, using this tool earlier on it would have prevented these mistakes and quickened the workflow.

Finally the devising of a rigorous test procedure with very specific and progressive steps helped immensely with the debugging of the board by progressively eliminating possible causes of failure. In consequence I highly recommend that any future PCB for N-Pulse follow a similar test program.

Future work

Apart from carrying out the test program to the end and correcting the mistakes which have been discovered in the process, the next step for N-Pulse is to integrate the ELEA board in an EMG Bracelet proof-of-concept, implement the classifier software and evaluate the performance of the system.

From there, a second version of the Signal Processing board can be developed based on the experience of the first one. Some important things to consider are :

- characterize the performance of the three antennas to see which one suits our application the most (or replace with an antenna-integrated RF module if none work appropriately)
- decide if the EMG Bracelet will use BioAMP or custom signal acquisition modules to reduce the complexity of the power delivery section
- verify if any MCU integrating USB On-The-Go capability appropriately fulfills the requirements, allowing to get rid of the MCP2200 chip and its large crystal

Since minimizing the footprint of current version of the Signal Processing board (ELEA) was not a priority, just these three steps and closer placement of components will reduce the board area by a factor of two or three allowing to integrate it in a proper, appropriately sized EMG Bracelet prototype.

Conclusion

This project successfully designed, assembled, and partially validated a custom, open-source signal processing PCB for the N-Pulse EMG Bracelet project, advancing the goal of a standalone, wearable, and intuitive prosthetic hand interface. The board was designed to handle 16 simultaneous EMG channels, power acquisition modules, and support onboard machine learning for gesture estimation, with both wired and wireless communication capabilities; however, these features require further validation after the end of this semester project. The iterative design process, careful component selection, and thorough documentation have established a robust foundation for future developments.

References

[1] ‘EPFL N-pulse’. Accessed: May 30, 2025. [Online]. Available: https://epfl-npulse.ch/

[2] ‘Electromyogram’, Physiopedia. Accessed: May 30, 2025. [Online]. Available: https://www.physio-pedia.com/Electromyogram

[3] B. Fatimah, P. Singh, A. Singhal, and R. B. Pachori, ‘Hand movement recognition from sEMG signals using Fourier decomposition method’, *Biocybern. Biomed. Eng.*, vol. 41, no. 2, pp. 690–703, Apr. 2021, doi: 10.1016/j.bbe.2021.03.004.

[4] K. H. Lee, J. Y. Min, and S. Byun, ‘Electromyogram-Based Classification of Hand and Finger Gestures Using Artificial Neural Networks’, *Sensors*, vol. 22, no. 1, p. 225, Dec. 2021, doi: 10.3390/s22010225.

[5] S. Ni, M. A. A. Al-qaness, A. Hawbani, D. Al-Alimi, M. Abd Elaziz, and A. A. Ewees, ‘A survey on hand gesture recognition based on surface electromyography: Fundamentals, methods, applications, challenges and future trends’, *Appl. Soft Comput.*, vol. 166, p. 112235, Nov. 2024, doi: 10.1016/j.asoc.2024.112235.

[6] ‘Surface EMG: An Exciting New Form of HCI That Considers Everyone’. Accessed: May 30, 2025. [Online]. Available: https://www.meta.com/blog/quest/surface-emg-wristband-electromyography-human-computer-interaction-hci

[7] *N-Pulse/EMG-HW-SigAcq*. (Mar. 16, 2025). HTML. N-Pulse. Accessed: Jun. 05, 2025. [Online]. Available: https://github.com/N-Pulse/EMG-HW-SigAcq

[8] F. Rossi, A. Mongardi, P. M. Ros, M. R. Roch, M. Martina, and D. Demarchi, ‘Tutorial: A Versatile Bio-Inspired System for Processing and Transmission of Muscular Information’, *IEEE Sens. J.*, vol. 21, no. 20, pp. 22285–22303, Oct. 2021, doi: 10.1109/JSEN.2021.3103608.

[9] A. Mongardi *et al.*, ‘Hand Gestures Recognition for Human-Machine Interfaces: A Low-Power Bio-Inspired Armband’, *IEEE Trans. Biomed. Circuits Syst.*, vol. 16, no. 6, pp. 1348–1365, Dec. 2022, doi: 10.1109/TBCAS.2022.3211424.

[10] ‘(PDF) Technical Features and Functionalities of Myo Armband: An Overview on Related Literature and Advanced Applications of Myoelectric Armbands Mainly Focused on Arm Prostheses’, *ResearchGate*, Feb. 2025, doi: 10.21307/ijssis-2018-005.

[11] S. Rawat, S. Vats, and P. Kumar, ‘Evaluating and exploring the MYO ARMBAND’, in *2016 International Conference System Modeling & Advancement in Research Trends (SMART)*, Nov. 2016, pp. 115–120. doi: 10.1109/SYSMART.2016.7894501.

[12] I. Mendez *et al.*, ‘Evaluation of the Myo armband for the classification of hand motions’, in *2017 International Conference on Rehabilitation Robotics (ICORR)*, Jul. 2017, pp. 1211–1214. doi: 10.1109/ICORR.2017.8009414.

[13] C. Tepe and M. Erdim, ‘Classification of surface electromyography and gyroscopic signals of finger gestures acquired by Myo armband using machine learning methods’, *Biomed. Signal Process. Control*, vol. 75, p. 103588, May 2022, doi: 10.1016/j.bspc.2022.103588.

[14] K. E. Yu *et al.*, ‘Clinical evaluation of the revolutionizing prosthetics modular prosthetic limb system for upper extremity amputees’, *Sci. Rep.*, vol. 11, p. 954, Jan. 2021, doi: 10.1038/s41598-020-79581-8.

[15] ‘Prosthetic Limb Reaches New Levels of Operability’, Quiet Corner. Accessed: Jun. 03, 2025. [Online]. Available: https://quiet-corner.com/prosthetic-limb-reaches-new-levels-operability/

[16] C. Indraccolo and L. T. De Paolis, ‘Augmented Reality and MYO for a Touchless Interaction with Virtual Organs’, in *Augmented Reality, Virtual Reality, and Computer Graphics*, L. T. De Paolis, P. Bourdot, and A. Mongelli, Eds., Cham: Springer International Publishing, 2017, pp. 63–73. doi: 10.1007/978-3-319-60928-7_6.

[17] J. Yao, ‘Developing a User-friendly System for Home-based Monitoring of Arm Use after Stroke’, *IMSAloquium Stud. Investig. Showc.*, Apr. 2025, [Online]. Available: https://digitalcommons.imsa.edu/sir_presentations/2025/Session3/27

[18] P. Zsoldos, B. Nagy, and F. P. Wijaya, 'Deep Learning-Based Implementation of Telerobotic Control with Gesture Recognition from EMG Signals', in *2025 11th International Conference on Automation, Robotics, and Applications (ICARA)*, Feb. 2025, pp. 6–10. doi: 10.1109/ICARA64554.2025.10977583.
[19] 'CTRL-kit', Curtis Barbre. Accessed: Jun. 03, 2025. [Online]. Available: https://www.curtisbarbre.com/ctrl-kit
[20] J. L. Betthauser *et al.*, 'Online Adaptation for Myographic Control of Natural Dexterous Hand and Finger Movements', Dec. 23, 2024, *arXiv*: arXiv:2412.17991. doi: 10.48550/arXiv.2412.17991.
[21] 'EMG Armband', Synchroni Scientific Instruments Inc. Accessed: Jun. 03, 2025. [Online]. Available: https://shop.synchroni.co/products/emg-armband
[22] 'uMyo - wearable EMG sensor', uDevices. Accessed: Jun. 04, 2025. [Online]. Available: https://udevices.io/products/umyo-wearable-emg-sensor
[23] 'MYO', Wearables.com. Accessed: Jun. 06, 2025. [Online]. Available: https://wearables.com/products/myo
[24] VR Trailers & Clips, *Facebook's Wrist-Worn Neural Finger Tracking Prototype In Action*, (Mar. 18, 2021). Accessed: Jun. 06, 2025. [Online Video]. Available: https://www.youtube.com/watch?v=WmxLiXAo9ko
[25] 'Batterie LiPo Tattu R-Line 2S 550mAh (XT30)', studioSPORT. Accessed: Jun. 05, 2025. [Online]. Available: https://www.studiosport.fr/batterie-lipo-r-line-2s-550mah-xt30-tattu-a26134.html
[26] 'BioAmp EXG Pill — upsidedownlabs.github.io documentation'. Accessed: May 30, 2025. [Online]. Available: https://docs.upsidedownlabs.tech/hardware/bioamp/bioamp-exg-pill/index.html
[27] 'The Nyquist–Shannon Theorem: Understanding Sampled Systems - Technical Articles'. Accessed: Jun. 05, 2025. [Online]. Available: https://www.allaboutcircuits.com/technical-articles/nyquist-shannon-theorem-understanding-sampled-systems/
[28] S. Muceli and R. Merletti, 'Tutorial. Frequency analysis of the surface EMG signal: Best practices', *J. Electromyogr. Kinesiol.*, vol. 79, p. 102937, Dec. 2024, doi: 10.1016/j.jelekin.2024.102937.
[29] M. Kalbasi, M. Shaeri, V. A. Mendez, S. Shokur, S. Micera, and M. Shoaran, 'A Hardware-Efficient EMG Decoder with an Attractor-based Neural Network for Next-Generation Hand Prostheses', in *2024 IEEE 6th International Conference on AI Circuits and Systems (AICAS)*, Apr. 2024, pp. 532–536. doi: 10.1109/AICAS59952.2024.10595960.
[30] 'A Guide to Hand-Calculating FLOPs and MACs | by Pasha Shaik | Medium'. Accessed: May 30, 2025. [Online]. Available: https://medium.com/@pashashaik/a-guide-to-hand-calculating-flops-and-macs-fa5221ce5ccc
[31] 'ANT-2.4-PML-UFL : Antennas', TE Connectivity. Accessed: Jun. 06, 2025. [Online]. Available: https://www.te.com/en/product-L9000097-01.html
[32] R. Traiger, 'Matching service optimizes GSM-900, WiFi, Bluetooth, GPS/GNSS, ZigBee, 4G/LTE antenna placement', Analog IC Tips. Accessed: Jun. 06, 2025. [Online]. Available: https://www.analogictips.com/matching-service-optimizes-gsm-900-wifi-bluetooth-gps-gnss-zigbee-4g-lte-antenna-placement/
[33] 'Pin header', *Wikipedia*. Apr. 05, 2025. Accessed: Jun. 06, 2025. [Online]. Available: https://en.wikipedia.org/w/index.php?title=Pin_header&oldid=1284077356
[34] 'Fabricant de prototypes PCB et de fabrication PCB - JLCPCB'. Accessed: May 31, 2025. [Online]. Available: https://jlcpcb.com/fr
[35] 'Controlled Impedance PCB Layer Stackup- JLCPCB'. Accessed: Jun. 01, 2025. [Online]. Available: https://jlcpcb.com/impedance
[36] 'Datasheet - STM32WBA6xxx'. Accessed: May 31, 2025. [Online]. Available: https://www.st.com/resource/en/datasheet/stm32wba62ci.pdf
[37] 'esp32-s3-wroom-1_wroom-1u_datasheet_en.pdf'. Accessed: May 31, 2025. [Online]. Available: https://www.espressif.com/sites/default/files/documentation/esp32-s3-wroom-1_wroom-1u_datasheet_en.pdf
[38] 'ads7953.pdf'. Accessed: May 31, 2025. [Online]. Available: https://www.ti.com/lit/ds/symlink/ads7953.pdf?ts=1747339663879&ref_url=https%253A%252F

%252Fwww.ti.com%252Fproduct%252FADS7953%252Fpart-details%252FADS7953SBRHBR%253FHQS%253Docb-tistore-invf-invftransact-invf-store-octopart-wwe
[39] 'REF50xx Low-Noise, Very Low Drift, Wide VIN Precision Voltage Reference'. Accessed: May 31, 2025. [Online]. Available: https://www.ti.com/lit/ds/symlink/ref50.pdf?ts=1748686177162&ref_url=https%253A%252F%252Fwww.mouser.fr%252F
[40] 'OPAx192 36-V, Precision, Rail-to-Rail Input/Output, Low Offset Voltage, Low Input Bias Current Op Amp with e-trim'. Accessed: May 31, 2025. [Online]. Available: https://www.ti.com/lit/ds/symlink/opa4192.pdf?ts=1748674968949
[41] 'MCP2200 : USB 2.0 to UART Protocol Converter with GPIO'. Accessed: May 31, 2025. [Online]. Available: https://ww1.microchip.com/downloads/en/DeviceDoc/22228A.pdf
[42] M. Afaneh, 'Bluetooth Low Energy (BLE): A Complete Guide', Novel Bits. Accessed: Jun. 01, 2025. [Online]. Available: https://novelbits.io/bluetooth-low-energy-ble-complete-guide
[43] 'Understanding Reflections and Standing Waves in RF Circuit Design | Real-Life RF Signals | Electronics Textbook'. Accessed: Jun. 01, 2025. [Online]. Available: https://www.allaboutcircuits.com/textbook/radio-frequency-analysis-design/real-life-rf-signals/understanding-reflections-and-standing-waves-rf-circuit-design/
[44] 'AN5165-How to develop RF hardware using STM32WB microcontrollers'. Accessed: Jun. 01, 2025. [Online]. Available: https://www.st.com/resource/en/application_note/an5165-development-of-rf-hardware-using-stm32wb-microcontrollers-stmicroelectronics.pdf
[45] 'Re: What is the output impedance of the STM32WBA63 (QFN48 package)'. Accessed: Jun. 01, 2025. [Online]. Available: https://community.st.com/t5/stm32-mcus-wireless/what-is-the-output-impedance-of-the-stm32wba63-qfn48-package/td-p/792900
[46] 'Pi-Matching Impedance Network Calculator'. Accessed: Jun. 06, 2025. [Online]. Available: https://www.elektroda.com/calculators/impedance-circuit-solver-pi-match
[47] 'BGS13SN8E6327XTSA1 Infineon Technologies | Mouser', Mouser Electronics. Accessed: Jun. 06, 2025. [Online]. Available: https://eu.mouser.com/ProductDetail/Infineon-Technologies/BGS13SN8E6327XTSA1?qs=0DP5yvOrqYmFtfP%252BZ8kQgQ%3D%3D
[48] 'FXUB63.07.0150C Taoglas | Mouser', Mouser Electronics. Accessed: Jun. 06, 2025. [Online]. Available: https://www.mouser.fr/ProductDetail/Taoglas/FXUB63.07.0150C?qs=gQGbhTXPkfjmZD6VcqXhgg%3D%3D
[49] 'AMCA31-2R450G-S1F-T3.pdf'. Accessed: Jun. 06, 2025. [Online]. Available: https://abracon.com/chip-antenna/AMCA31-2R450G-S1F-T3.pdf
[50] A. Andersen, 'AN043 - Small Size 2.4 GHz PCB antenna'.
[51] 'SWRC062 Support software | TI.com'. Accessed: Jun. 01, 2025. [Online]. Available: https://www.ti.com/tool/download/SWRC062
[52] 'STM32CubeIDE - Integrated Development Environment for STM32 - STMicroelectronics'. Accessed: Jun. 05, 2025. [Online]. Available: https://www.st.com/en/development-tools/stm32cubeide.html
[53] 'STM32CubeProg - STM32CubeProgrammer software for all STM32 - STMicroelectronics'. [Online]. Available: https://www.st.com/en/development-tools/stm32cubeprog.html

Annexes

Plans

The complete project can be accessed at : https://github.com/N-Pulse/EMG-HW-MainBoard

Images of the schematics and layout are given in the following

Schematics

Screenshots of each of the hierarchical sheets of the schematic made in KiCAD schematic editor.

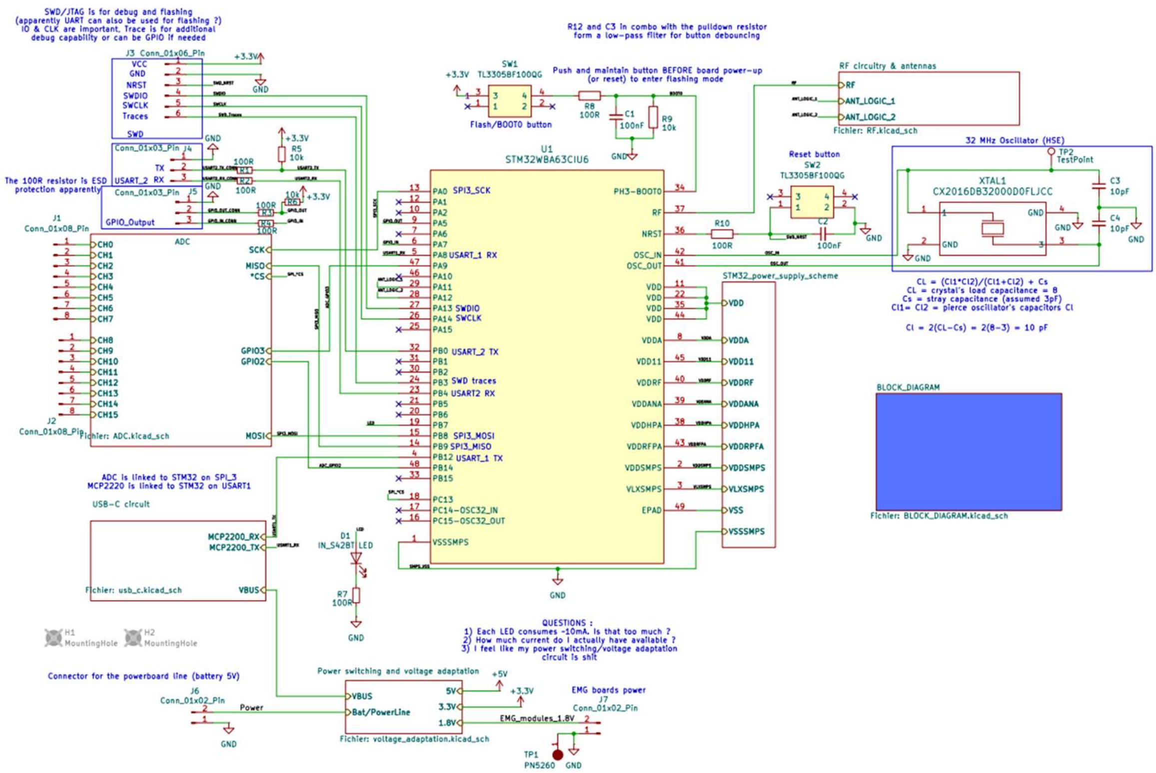

Figure 21 : Root schematic sheet

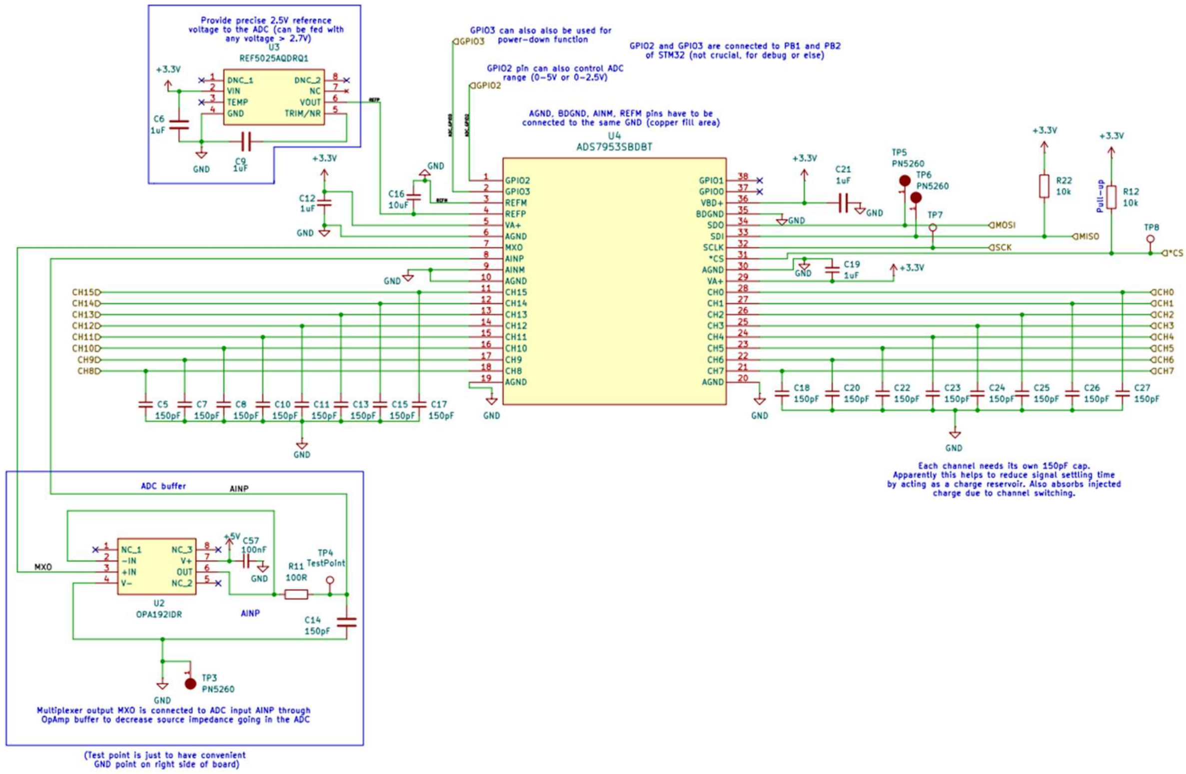

Figure 22 : ADC subsytem schematic sheet

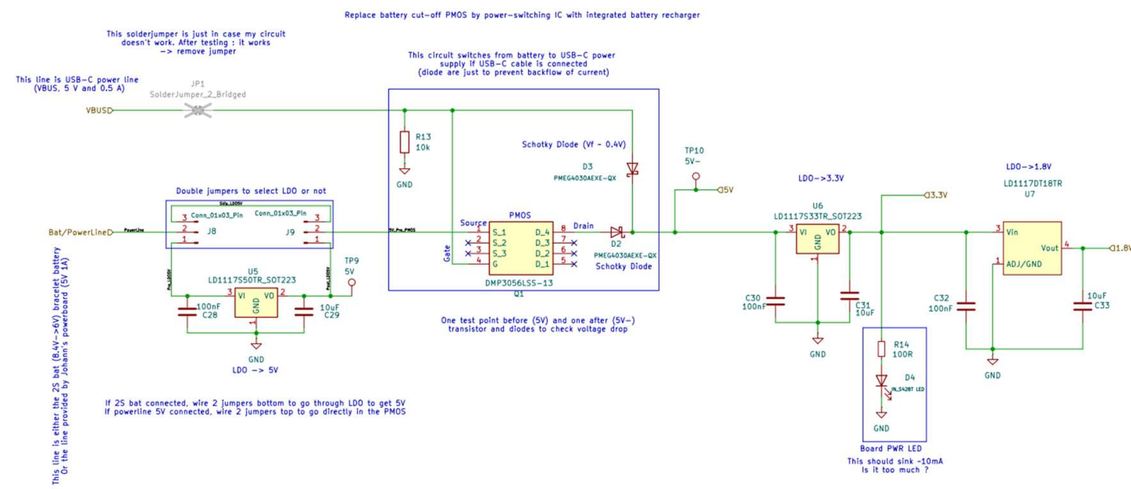

Figure 23 : Power section schematic sheet

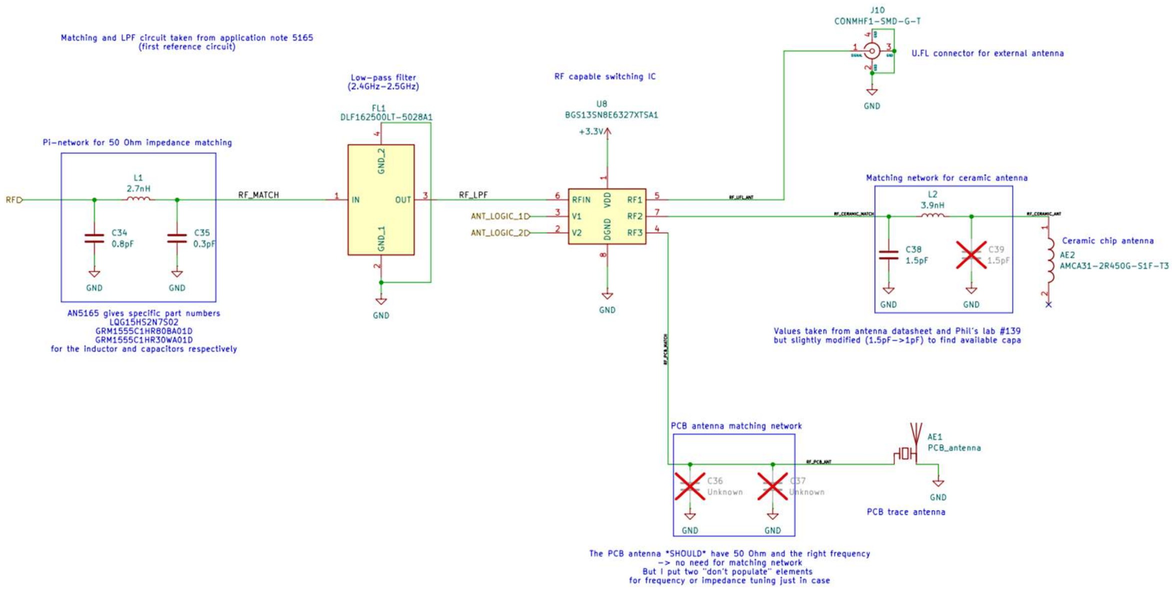

Figure 24 : RF section schematic sheet

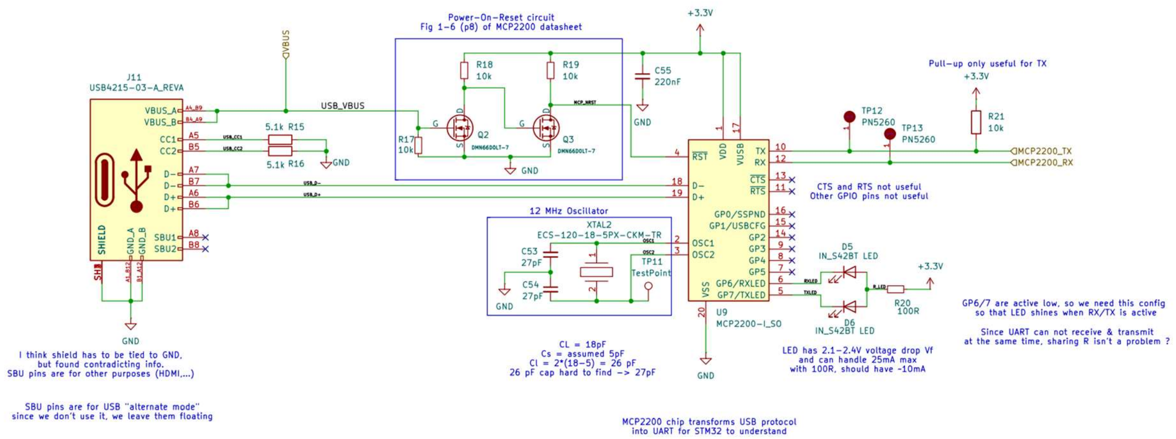

Figure 25 : USB section schematic sheet

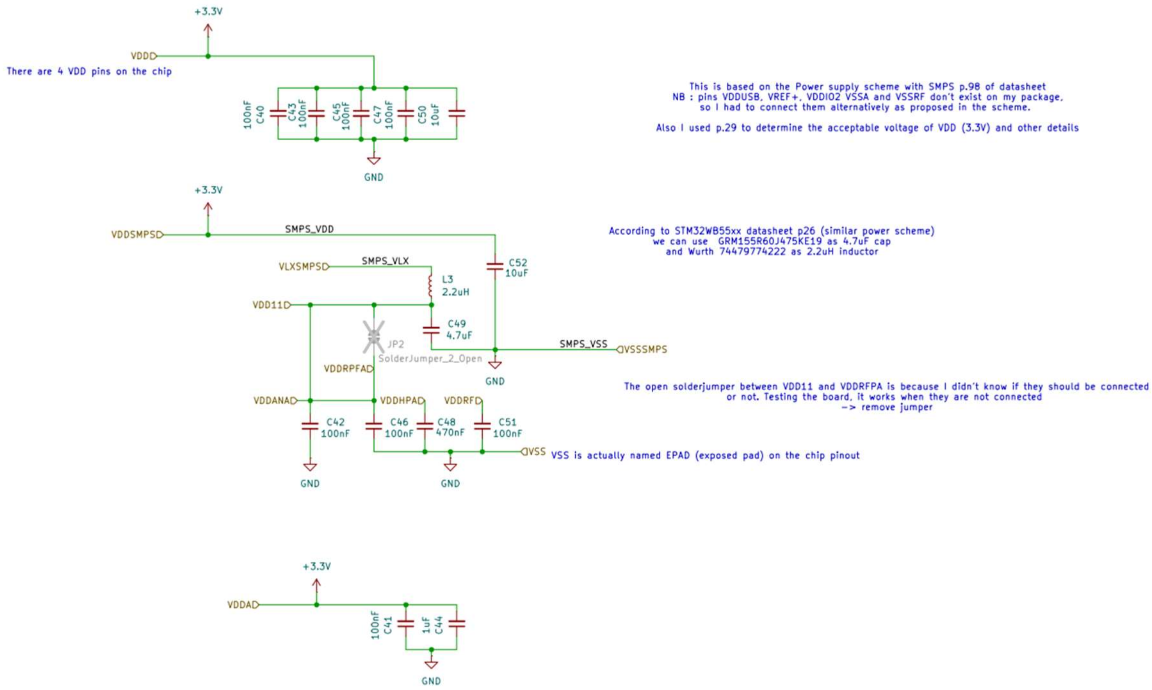

Figure 26 : STM32's decoupling capacitors

Plane layout

Here are screenshots from KiCAD layout editor to illustrate the overall layout of the board and the different planes

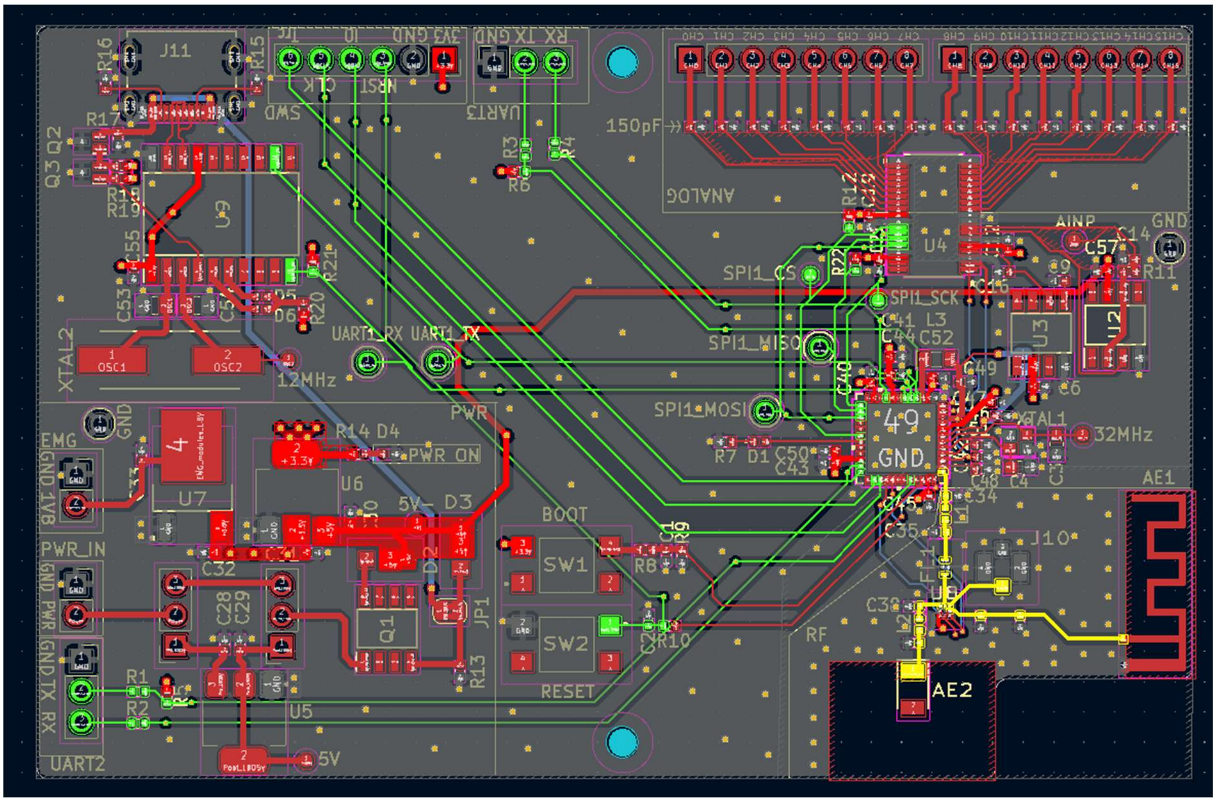

Figure 27 : Functionnal layout overview (combination of top, bottom, silkscreen and component courtyard layers)

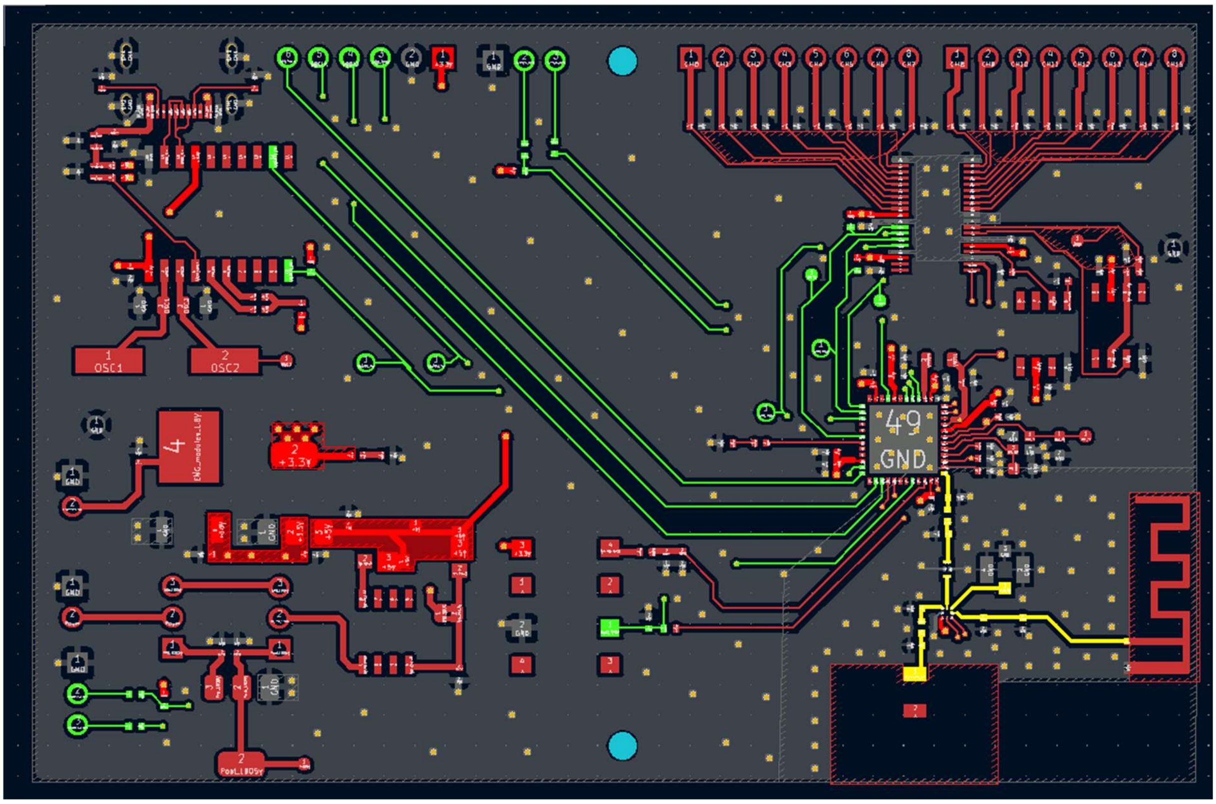

Figure 28 : Top plane (Grey : GND, light red : 3V3 or 5V, Yellow : Controlled Impedance 50 Ohm, green : USART/SPI, dim red : other)

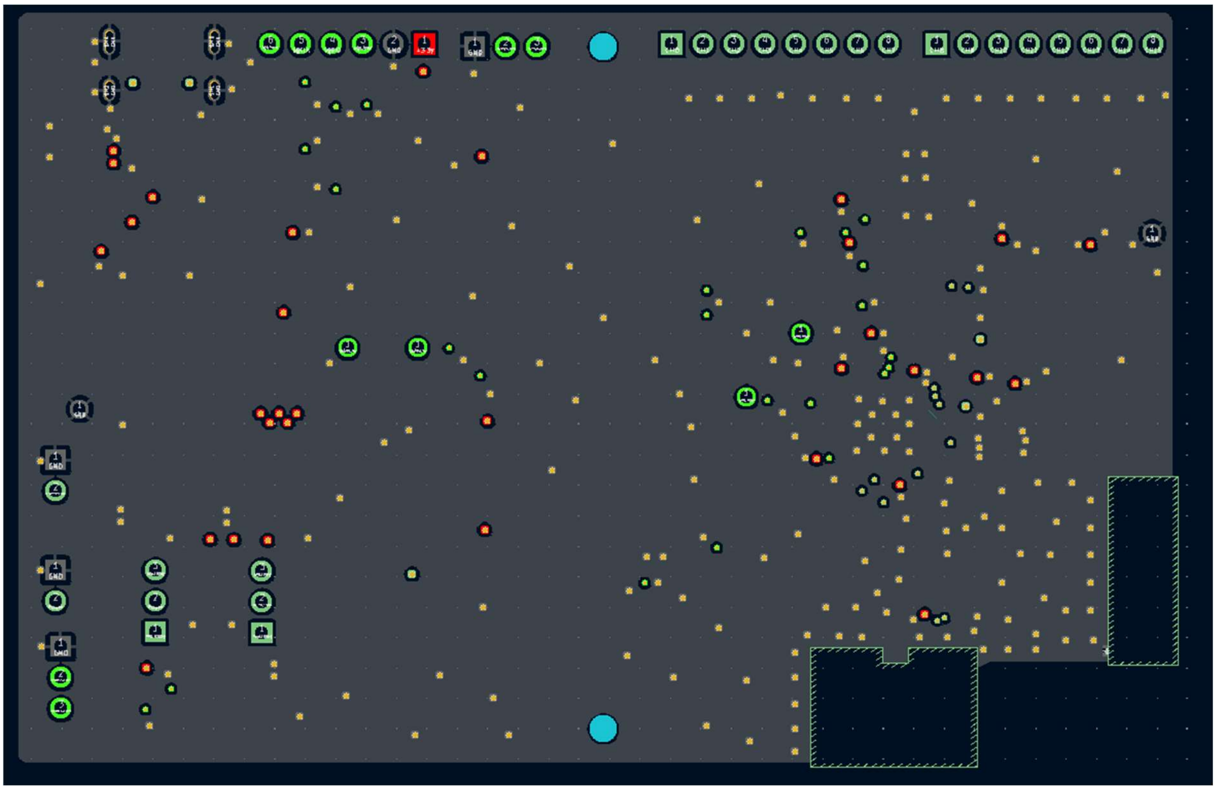

Figure 29 : 2nd plane (GND)

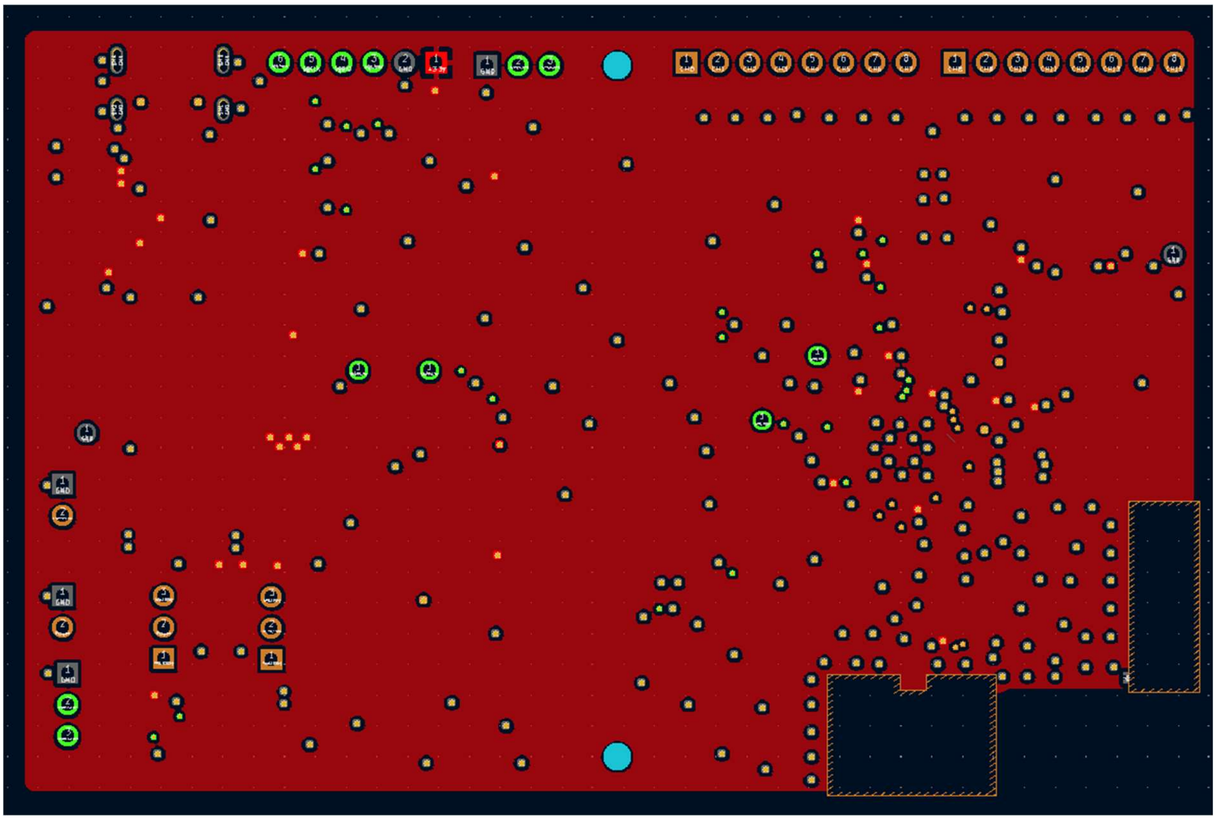

Figure 30 : 3rd plane (3V3)

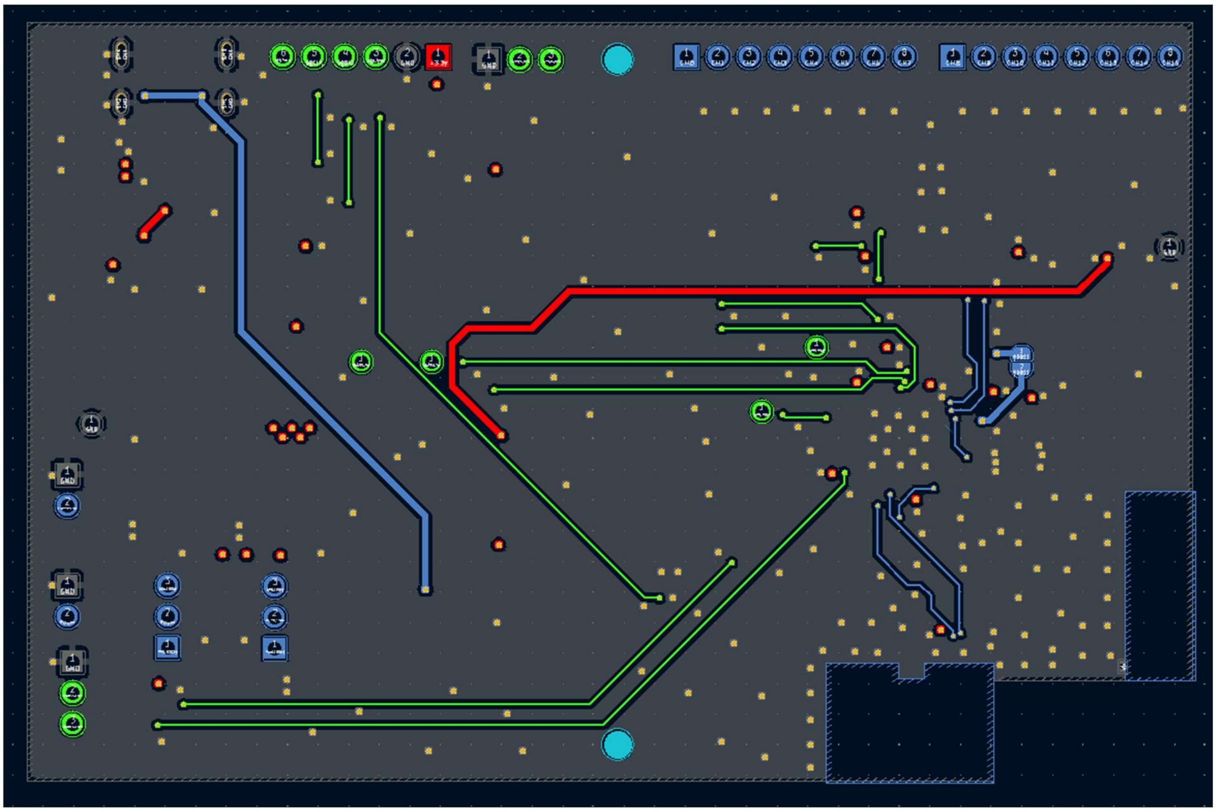

Figure 31 : 4th plane (green : USART/SPI, light red : 3V3 or 5V, blue : other)

Tutorial

Useful resources

Here is a list of online resources where I learned most of what I know.

- Phil's lab (https://www.youtube.com/@PhilsLab): the youtube channel of a PCB design expert, has tons of extremely in-depth tutorials on making a PCB from start to finish (STM32CubeIDE, datasheet comprehension, Kicad, schematic design and layout). He taught me everything. A lot of this PCB was inspired by his videos #127 and #128.
- Altium Academy (https://www.youtube.com/@AltiumAcademy) : educational channel of Altium (pro version of Kicad essentially)
- Electronics stack exchange (https://electronics.stackexchange.com/) : great place to ask questions and get answers. Level of detail of the answer depends, but it often helps
- ST community forum (https://community.st.com/) : longer response time but more precise and involved help. Can get answers from actual ST engineers.
- All about circuits has generally very useful articles about many electronic engineering subjects : https://www.allaboutcircuits.com/
- DeepBlueEmbedded has very complete (but not always noob friendly) tutorials, especially for STM32 : https://deepbluembedded.com/

Here are also some good sources for some specific topics.

USB-C :
https://dubiouscreations.com/2021/04/06/designing-with-usb-c-lessons-learned/
https://microchip.my.site.com/s/article/USB-Type-C-Layout-Recommendations

Impedance control :
https://www.allaboutcircuits.com/textbook/radio-frequency-analysis-design/real-life-rf-signals/the-50-question-impedance-matching-in-rf-design/
https://www.wevolver.com/article/controlled-impedance

Mini crash course on antennas :
https://colinkarpfinger.com/blog/2010/the-dropouts-guide-to-antenna-design/

The STM32 clock system :
https://community.st.com/t5/stm32-mcus/part-1-introduction-to-the-stm32-microcontroller-clock-system/ta-p/605369

A wiki for for STM32:
https://stm32world.com/wiki/Main_Page

Improvements for next version

Power Management

* Replace the current PMOS-based power circuit with a dedicated power switching IC. This should improve reliability and can also integrate a USB battery charging system, eliminating the need to charge the battery externally.

* If using only custom EMG modules (which output up to \~1.8V), power the op-amp with 3.3V (V+ = 3.3V, V– = GND) instead of 5V. This allows:

  * Removal of the 5V LDO

  * Use of a 1S battery (3.0V–4.2V) instead of 2S

  * Simplification of the power circuit (e.g., use Theo's original circuit with modified G and S).

Op-Amp Buffer for ADC

* Reevaluate the need for the op-amp buffer on the ADC input:

  * Check ADC datasheet (e.g., page 50) for unbuffered mode operation and source impedance requirements.

  * Option 1: Measure the output impedance of the EMG module (was attempted but not successful—could try again).

  * Option 2: Empirically test ADC performance (sample rate and signal fidelity) with and without the buffer.

* Even if not ideal, the ADC's max rate is 1 MSps, and we only need \~100 kSps (16 channels × 800 Hz, with margin), so removing the op-amp may be acceptable and desirable (fewer components, cost, and no need for 5V).

Voltage Regulators

* Replace the 1.8V LDO with a version in SOT-223 package (e.g., LD1117S18TR_SOT223) to match the others and simplify footprint management in KiCad. It's also easier to find in libraries.

ESD and Debug Interface

* Consider adding ESD protection between the USB port and the rest of the board.

* If board height is a constraint, use a TAG-Connect-style connector for SWD/debug lines (as seen in Phil's Lab #127) to reduce profile.

Bypass Capacitors

* Replace all 100nF bypass capacitors with 1µF capacitors. Based on modern decoupling practices, this offers better performance:

  [Proper decoupling practices – CodeInSecurity](https://codeinsecurity.wordpress.com/2025/01/25/proper-decoupling-practices-and-why-you-should-leave-100nf-behind/)

RF & Antenna Design

* If antenna performance is insufficient, consider switching to the ESP32-S3-WROOM-1 module, which includes an integrated antenna and validated RF layout. Pros:

  * Reliable RF performance

  * Ready-to-use KiCad footprint

  * Simplified layout (antenna, crystal, decoupling already included)

  * Software workload increases (interfacing with second MCU or flashing)

* If using ESP32-S3-WROOM-1, reevaluate the need for a radio-capable STM32. Instead, prioritize:

  * Adequate Flash, RAM, and clock for the ML workload (e.g., STM32WBA3CI has 2MB Flash)

  * Native USB (to remove MCP2200 chip)

  * SPI for ADC communication

  * At least one UART for communication with Daniel's board

  > Note: This is a **major architecture change**, only pursue if clearly beneficial.

MCU Considerations

* Investigate whether STM32WBA65 is a better fit. Advantages:

  * Native USB support (USB On-The-Go)

  * Similar to the current MCU, minimal rework

  * Can eliminate MCP2200 chip and its crystal

  * See datasheet p.14 for function comparison

* If going with a new MCU, also explore modules with integrated antennas (e.g., from ST or Espressif) to simplify RF, decoupling, and crystal requirements.

RF Impedance Matching

* Recalculate impedance matching network near the STM32 RF pin using correct values:

  * From ST forums: Z = 22.7 – j9.3, Q = 5 (to confirm)

  * Calculated values: L = 1.09 nH, CS = 6.63 pF, CL = 7.92 pF

  * These differ slightly from current design, but the correct values were found too late for this revision.

Connector Optimization

* Consider removing GPIO connector J5 and freeing up pins PA5 and PA7 (UART3 isn't available on STM32WBA63, making them redundant).

 * At the very least, remove external pull-ups since GPIOs have internal configurable pull resistors.

Miscellaneous Hardware Changes

* Remove JP2 (open solder bridge jumper) — VDD11 and VDDRFPA should be isolated.

* Remove JP1 — USB power cutoff circuit (Theo's adapted design) is functional.

* Remove the boot button — it's only used to trigger the firmware bootloader, which is rarely necessary.

    * If needed, expose a pad (e.g., via open solder jumper) to manually pull BOOT to 3.3V.

* Add more test points, especially small exposed pads:

  * Use vias to place them on the bottom layer if top layer space is limited.

  * Example: had one at OPA192 output; should have added one at the input too.

Collection of design notes

Crystal Capacitor Selection

* Stray capacitance (Cs) is typically 3–5 pF; I usually assume 4 pF.

* For the STM32 HSE, the calculated load capacitance was 8 pF. However, since 8 pF capacitors are hard to source, I adjusted the Cs assumption to 3 pF, resulting in a 10 pF capacitor value, which is easier to find.

* STM32 includes internal capacitor banks on HSE oscillator pins, which can be configured via software (registers) to fine-tune frequency.

Controlled Impedance Traces

* Based on AN043 board files:

  * Coplanar single-ended layout

  * Trace width: 0.43 mm, spacing to ground pour: 0.36 mm

  * 4-layer board: copper layers 0.035 mm thick, dielectric stack: top 0.25 mm, mid 0.5 mm, bottom 0.25 mm (1.2 mm total thickness)

* Using AppCAD (coplanar waveguide tool):

  * For H = 0.25 mm, T = 0.035 mm, G = 0.36 mm, W = 0.456 mm for 50 Ohm

  * Alternate config: G = 0.35 mm, T = 0.453 mm

* JLCPCB's impedance calculator:

  * Closest match: JLC041211-7628B (expensive)

  * Cheaper but less accurate: JLC041211-7628

USB Differential Pair

* USB-C uses differential signals (D+ and D–)

* Differential impedance control is critical only for high-speed protocols (e.g., USB 2.0 High Speed).

* For USB 1.1 Full Speed, traces must be >17 cm to require impedance matching (see [StackExchange post](https://electronics.stackexchange.com/questions/743303/...))

RF Impedance Matching

* RF output pin is not 50 Ohm matched

* Used AN5165 (for STM32WB55) as reference initially

* Later found correct impedance values for STM32WBA63: Z = 22.7 – j9.3, Q = 5

* Pi-matching calculator results: L = 1.09 nH, CS = 6.63 pF, CL = 7.92 pF

* Didn't update the BOM in time to match those exact values

RF Antenna Compatibility

* Roman's antenna (Taoglas FXUB63.07.0150C) supports 2.4 GHz Wi-Fi, ISM, and AGPS

* BLE also uses 2.4 GHz, so likely compatible, though not explicitly stated in the datasheet

SPI Design Notes

* Refer to Phil's Lab #134 for SPI basics

* Pull-ups not needed for SPI, but a pull-up on CS line is recommended

* Add 0–22 Ohm series resistors on CLK line as placeholders for termination

UART Design Notes

* Pull-up on TX line may be beneficial ([StackExchange source](https://electronics.stackexchange.com/questions/270834/...)), though not critical

PCB Reannotation Warning

* Do NOT use the auto-reannotate tool after laying out the PCB—will mess up component names, requiring manual fix

BioAMP EXG Pill Support

* Design intended to support both custom and BioAMP modules
* Missing 5V output for BioAMPs can be worked around:
  * With 2S battery: set jumpers to pass through 5V LDO
  * Use triple pin header to bridge J9 pins -> pin 3 of J8 becomes 5V output
  * With 5V power source: use same source for BioAMP; set jumpers to bypass LDO

Oscillator Tuning

* STM32WB series has internal capacitance banks on OSC_IN/OSC_OUT
* Can potentially fine-tune or even replace external capacitors CL1/CL2 via RCC_ECSCR1 register
* See app note: "How to calibrate the HSE clock for RF applications on STM32 wireless MCUs"
* Also, see [DeepBlueEmbedded tutorial](https://deepbluembedded.com/stm32-rcc-clock-configuration-ultimate-guide/) for clock configuration in CubeIDE

Additional SPI Resources

* [DeepBlueEmbedded STM32 SPI Tutorial](https://deepbluembedded.com/stm32-spi-tutorial/)
* [StackExchange post on SPI termination](https://electronics.stackexchange.com/questions/234703/...)

USART Configuration

* USART3 does NOT exist on STM32WBA63
* Enable interrupts on USART2 (for external comms);

Flash / Boot Notes

* Refer to "AN2606 STM32 microcontroller system memory boot mode"

* Programming likely via SWD/JTAG:

    * SWDIO on PA13, SWDCLK on PA14

* PH3-BOOT0 logic:

    * On first boot, checks if flash is blank

  * If blank, activates bootloader; otherwise runs user code

  * Tie BOOT0 to GND; leave optional pad/jumper for forcing boot mode manually

NRST Pin

* Used to reset MCU; should connect to a momentary switch

* Triggers bootloader when flashing via communication channels or resets MCU when SWD unavailable

* [StackExchange NRST use case](https://electronics.stackexchange.com/questions/491068/...)

BLE / RF Component Choice

* Originally referenced Phil's Lab #127

* For chip antenna, tried component from AN5434 section 3.8

  * Datasheet link was broken; used ST forum (thanks Remi!)

  * Ultimately chose same antenna as Phil's Lab #127 for better documentation

* Reference: [STM32WBA65I-DK1 Eval Board](https://www.st.com/en/evaluation-tools/stm32wba65i-dk1.html#overview)

STM32CubeIDE for Design Planning

* Initially assumed 3 UARTs; discovered only 2 when configuring in CubeIDE

* Resolved by assigning extra UART pins as GPIO (PA5 as output, PA7 as input)

* Tip: Use STM32CubeIDE early in design to plan pinout instead of relying only on datasheets

* Also discovered SPI3 has limitations (only 8/16-bit transfers, max 1024 data points)

* Tip: Use Ctrl + Left Click on function pin to highlight all related pins

Handling Unused Pins

* Options for unused STM32 pins:

  * Define as GPIO Input with pulldown resistor
  * Leave floating only if explicitly supported
* References:

  * [Unused pins StackExchange #1](https://electronics.stackexchange.com/questions/719319/...)
  * [Unused pins StackExchange #2](https://electronics.stackexchange.com/questions/50539/...)